ELSEVIER

Chemical Geology 241 (2007) 177–206

CHEMICAL GEOLOGY
INCLUDING
ISOTOPE GEOSCIENCE

www.elsevier.com/locate/chemgeo

Ambient and excess mantle temperatures, olivine thermometry, and active vs. passive upwelling

Keith D. Putirka [a,*], Michael Perfit [b], F.J. Ryerson [c], Matthew G. Jackson [d]

[a] California State University, Fresno, Department of Earth and Environmental Sciences, 2576 E. San Ramon Ave., MS/ST24, Fresno, CA 93710, USA
[b] University of Florida, Department of Geological Sciences, Box 112120, Gainesville, FL 32611-2120, USA
[c] Lawrence Livermore National Laboratory, Institute of Geophysics and Planetary Physics, L-206, Livermore, CA 94550, USA
[d] MIT-Woods Hole Oceanographic Institution Joint Program, Woods Hole, MA, 02543, USA

Accepted 22 January 2007

Abstract

Mantle temperatures provide a key test of the mantle plume hypothesis, and olivine-liquid equilibria provide perhaps the most certain means of estimating mantle temperatures. Here, we review mantle temperature estimates and olivine thermometers, and calculate a new convective geotherm for the upper mantle. The convective geotherm is determined from estimates of sub-mid-ocean ridge (MOR) mantle potential temperatures (T_p is the T the mantle would have if it rose adiabatically without melting, and provides a reference for measuring excess temperatures at volcanic hot spots; $T_{ex} = T_p^{hot\ spot} - T_p^{MOR}$). The Siqueiros Transform has high MgO glass compositions that have been affected only by olivine fractionation, and yields $T_p^{Siqueiros} = 1441 \pm 63$ °C. Most mid-ocean ridge basalts (MORB) have slightly higher FeO^{liq} than at Siqueiros; if Fo_{max} (=91.5) and Fe^{2+}–Mg exchange at Siqueiros apply globally, then upper mantle T_p is closer to 1466 ± 59 °C. Since our global MORB database was not filtered for hot spots besides Iceland, Siqueiros may in fact be representative of ambient mantle, so we average these estimates to obtain $T_p^{MOR} = 1454 \pm 81$ °C; this value is used to calculate T_{ex}. Global MORB variations in FeO^{liq} indicate that 95% of the sub-MORB mantle has a global T range of ±140 °C; 68% of this range (1σ) exhibits temperature variations of ±34 °C. Our estimate for T_p^{MOR} defines the convective mantle geotherm; this estimate is consistent with T estimates from sea floor bathymetry, and overlaps within 1σ estimates derived from phase transitions at the 410 km and 670 km seismic discontinuities. Mantle potential temperatures at Hawaii and Samoa are identical at 1722 °C and at Iceland is 1616 °C; hence T_{ex} is ≈268 °C at Hawaii and Samoa and 162 °C at Iceland. Furthermore, T_p estimates at Hawaii and Samoa exceed maximum T_p estimates at MORs by >100 °C. Our T_{ex} estimates agree with estimates based on excess topography and dynamic models of mantle flow and melt generation. Rayleigh number calculations further show that if our values for T_{ex} extend to depths as small as 135 km, thermally driven, active upwellings will ensue. Hawaii, Samoa and Iceland thus almost assuredly result from thermally driven active upwellings, or mantle plumes. Estimates of T_{ex} account for generalized differences in H_2O contents between ocean islands and MORs, and are robust against variations in CO_2, and major element components, and thus cannot be explained away by the presence of volatiles or more fusible source materials. However, our temperature variations at MORs do not account for H_2O variations within the MORB source region.

Keywords: Mantle plumes; Hot spots; Thermometry; Olivine; Geothermal gradient; Mid-ocean ridge

1. Overview

The recent debate over the existence of mantle plumes has to some extent strayed from a fundamental issue: Do

* Corresponding author.
E-mail addresses: kputirka@csufresno.edu (K.D. Putirka), perfit@geology.ufl.edu (M. Perfit), ryerson1@llnl.gov (F.J. Ryerson), mjackson@whoi.edu (M.G. Jackson).

0009-2541/$ - see front matter © 2007 Elsevier B.V. All rights reserved.
doi:10.1016/j.chemgeo.2007.01.014

mid-plate volcanoes result from passive, or thermally driven active mantle upwelling? Morgan's (1971) plume proposal has two facets: 1) hot spots are the sites of active mantle upwelling and 2) the source of excess heat for thermal plumes is at the core mantle boundary. Much recent work has focused on part 2). For example, some suggest a core contribution to lavas from Hawaii (Brandon et al., 1999; Humayun et al., 2004), and Walker (2000) and Walker et al. (2002) have proposed several mechanisms for core–mantle mass transfer; a core contribution, though, is still unclear. Some have thus questioned the existence of thermally driven plumes with much attention given to seismic velocity anomalies, which can be interpreted as maps of temperature distributions. Some interpretations suggest that certain hot spots are connected to the core (e.g., Nataf and VanDecar, 1993; Wolfe et al., 1997; Montelli et al., 2004), while others suggest that thermal anomalies are confined to the upper mantle (e.g., Humphreys et al., 2000; Foulger et al., 2000; Christiansen et al., 2002). The debate has led to the proposal that all hot spots are shallow features—unconnected to narrow hot upwellings (Anderson, 1998; Foulger and Natland, 2003). But even if the core–mantle boundary was not the site of plume nucleation, a plume model might still be viable. The key issue is not whether the core contributes mass, or whether seismic low velocity anomalies are continuous from the surface to 2890 km, but rather: is there evidence that thermal anomalies exist? Thermally driven mantle plumes exist if hot spots can be shown to derive from thermally buoyant, "active" upwellings, as opposed to the passive mantle upwellings that give rise to mid-ocean ridge basalts. We suggest that the plume debate be recast to consider whether hot spots are sites of thermally driven active upwellings, and propose an observation-driven petrologic approach to identify mantle plumes.

Thermal upwellings, by definition, arise from sources with excess heat—and can be detected through estimates of "excess temperatures" from volcanic rocks. Anti-plume arguments lead to two significant implications: either (1) thermally buoyant upwelling currents do not exist or (2) such thermal currents have no impact on terrestrial volcanism. Alternative models for intra-plate volcanism include: lithospheric delamination (Foulger et al., 2005), small-scale passive mantle upwelling and lithosphere rifting (Christiansen et al., 2002), focusing of magma along lithosphere-scale cracks (Shaw and Jackson, 1973; Jackson et al., 1975), or compositional anomalies that depress the mantle solidus and promote partial melting (Bonatti, 1990; Green et al., 2001; Presnall and Gudfinnsson, 2005). In contrast to the thermal plume model, these models do not require a source of excess heat. If significant excess temperatures are not observed at "hot spots", then the thermally driven mantle plume model is likely to be incorrect, and these alternative models must be more vigorously explored.

In the discussion of T estimates, it is useful to have a conceptual reference, which McKenzie and Bickle (1988) provide in the form of a "mantle potential temperature", T_p. T_p represents the T a parcel of mantle would have if it were to rise to a planetary surface along an adiabat without melting (Fig. 1). Mantle potential temperatures thus reflect the "convective", as opposed to the conductive mantle geotherm. In regard to mantle melting, all parcels of mantle that have the same T_p, will intersect the solidus at the same depth, provided there are no differences in mantle composition. The most direct measure of "excess heat" is through identification of T_{ex}, a "mantle excess temperature." T_{ex} is the temperature difference between the core of a mantle melting anomaly, and surrounding ambient mantle ($T_{ex} = T_p^{\text{hot spot}} - T_p^{\text{AMG}}$; and because MORs are due to passive upwelling, $T_p^{\text{AMG}} = T_p^{\text{MOR}}$). The concept of T_{ex} is central to all thermal plume models, which require that (1) mantle excess temperatures provide sufficient thermal buoyancy to sustain active upwellings, and (2) that such thermal currents impinge the base of the lithosphere, and through their excess temperatures, give rise to sustained and voluminous volcanism, at random locations relative to plate boundaries. Whether the source of excess heat lies at the core–mantle boundary, the top of the lower mantle, or elsewhere, is important, but not decisive. If T_{ex} approaches zero at any particular hot spot the thermal plume model is likely incorrect at that locality, or at least not the exclusive mechanism for hot spot volcanism there. However, if T_{ex} can be shown to be significant at least at some hot spots, active upwellings, and hence plumes of some form, are likely to exist. Olivine thermometry is the most precise temperature measurement tool available to petrologists, which we apply to mid-ocean ridge basalts to delimit the sub-MOR mantle geotherm (henceforth referred to as the "average mantle geotherm" or AMG), and to Hawaii, Samoa and Iceland to test whether they derive from mantle sources with excess heat.

2. A review of some estimates of mantle temperatures

2.1. Prior T estimates of the sub-mid-ocean ridge (MOR) mantle

Alternatives to the plume model involve melting in the absence of a thermal perturbation. Opponents of the mantle plume hypothesis thus contend that T_{ex} ($= T_p^{\text{hot spot}} - T_p^{\text{ambient}}$) is small, on the order of tens of degrees C (Anderson, 1998; Foulger et al., 2005;

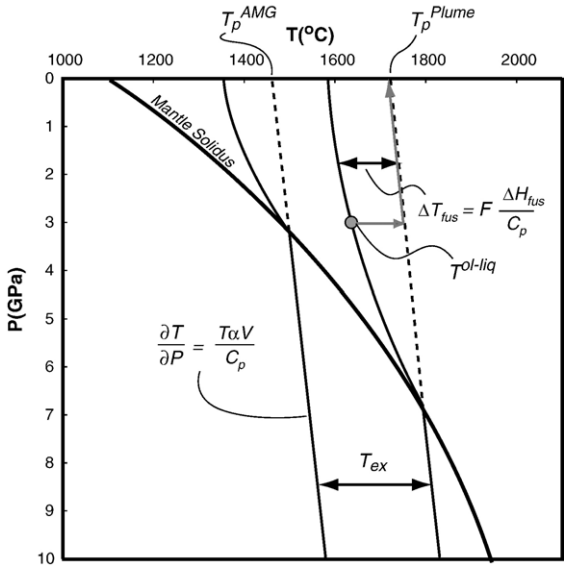

Fig. 1. The concepts of mantle potential (T_p) and excess (T_{ex}) temperatures are illustrated. In the plume hypothesis it is presumed that there is a source of excess heat, possibly at the core–mantle boundary, which gives rise to mid-plate volcanism. Regardless of where plumes nucleate, though, the plume model requires that T_p at hot spots (T_p^{Plume}) exceeds T_p for the average mantle geotherm, T_p^{AMG}. In contrast, alternative models to the mantle plume hypothesis require no excess heat, and hence predict that $T_{ex}=0$. Notice that in the absence of mantle heterogeneity, parcels of mantle that have the same T_p will intersect the mantle solidus at the same depths, while mantle plumes, with higher T_p must intersect the solidus at greater depths. Mantle potential temperatures and initial melting depths are thus intimately linked. The slope of the convective geotherm is presumed to be adiabatic, i.e., $\partial T/\partial P = T\alpha V/C_p$ (13.3 °C/GPa); where T is temperature, P is pressure, V is molar volume, α is the coefficient of thermal expansion, and C_p is heat capacity. Once a parcel of mantle intersects the solidus, energy is used to convert solid to liquid (Cawthorn, 1975); this results in a temperature drop that is approximated by $\Delta T_{fus} = F[\Delta H_{fus}/(C_p)]$, where ΔT_{fus} is the drop in temperature due to partial melting, F is the fraction of melt produced, and ΔH_{fus} is the heat of fusion. Cawthorn (1975) generates (as illustrated) curved lines to express the T drop upon fusion, as he considers $\Delta H_{fus} = f(T)$ and $C_p = f(T)$. Because error on F (see Appendix) is substantial, attempting to model such T-dependent behavior in the present instance, is clearly unwarranted. We thus apply constant values (ΔH_{fus} = 128.3 kJ/mole; C_p = 192.4 J/mole·K; $\alpha = 3\times10^{-5}$/K and V = 4.57 J/bar, see Putirka, 2005) to convert olivine-liquid equilibration temperatures (illustrated as a solid gray circle marked $T^{ol\text{-}liq}$) to T_p, through a two-step process ($T_p = T^{ol\text{-}liq} + \Delta T_{fus} - P[\partial T/\partial P]$; gray arrows).

Green and Falloon, 2005), or in the case of shear heating, possibly as high as 120 °C (Doglioni et al., 2005). But even when mantle compositions are well constrained, seismic estimates of temperature are uncertain. Precision ranges from ±100 °C in the upper mantle to ±250 °C in the lower mantle for a fixed mantle composition, and uncertainties increase to several hundreds of °C with as few as 0.5–1% differences in mineralogic models (Cammarano et al., 2003). Other seismic-mineral physics-based methods of T estimation derive from attempts to match mantle seismic discontinuities with phase transitions (e.g., Jeanloz and Morris, 1986). Such strategies provide only broad temperature limits, and are clouded by uncertainty in mantle composition, and consequent effects on phase transition boundaries (see Section 6); experiments by Hirose (2002), for example, cast doubt on inflection of the 670 km seismic discontinuity as a means to detect thermal anomalies.

Thermometry based on mantle partial melting is likely much more precise. Mantle temperature estimates appear to begin with Verhoogen (1954, 1965), followed by Green and Ringwood (1967) and Verhoogen (1973). Cawthorn (1975), though, presents the first clear analysis of mantle temperatures in the context of planetary volcanism, with a suggestion of excess temperatures at hot spots. Though Cawthorn's (1975) work predates McKenzie and Bickle's (1988) use of T_p, Cawthorn (1975) implicitly includes this concept, and quantified reductions in temperature that accompany partial melting. McKenzie (1984) provides the next advance; using parameterizations of the mantle solidus and liquidus, McKenzie varied T_p to predict crustal thicknesses at MORs. McKenzie and Bickle (1988) refined this strategy and proposed that T_p beneath MORs was 1280 °C. This value of 1280 °C has been much utilized since 1988, and Presnall et al. (2002) have recently estimated that T_p^{MOR} is between 1260–1310 °C. However, many independent analyses of T_p^{MOR} undertaken since 1988, based on crustal thickness and new experiments and thermodynamic models of mantle melting, yield much higher values for T_p^{MOR}: 1340–1475 °C (Kinzler and Grove, 1992b; Herzberg and O'Hara, 1998; Putirka, 1999; Asimow et al., 2001; Green et al., 2001; Wang et al., 2002; Herzberg, 2004; Putirka, 2005). The value for the average potential temperature beneath MORs is thus almost certainly much greater than 1280 °C, and more likely in the range of 1450±50 °C (Wang et al., 2002; Putirka, 2005). We test this idea further, by examining the global MORB database.

2.2. Prior estimates of T_{ex} and sub-MOR T variations

McKenzie (1967) appears to be the first to recognize that MORs result from passive upwelling, and the thermal consequences that ensue. Morgan (1971) built upon that insight, proposing that hot spots reflect active thermal upwellings, i.e., "plumes", implicitly recognizing that plumes should exhibit an excess temperature compared to MORs. Morgan (1971) also proposed that plumes

nucleate at the core–mantle boundary, though interestingly Hess (1962; his Fig. 8) appears to be the first to recognize that the core–mantle boundary may provide the thermal energy to drive active mantle upwellings; in this regard, the difference between Morgan (1971) and Hess (1962) is a matter of where upwellings impinge Earth's surface. In any case, McKenzie (1984) provided the first estimate of T_{ex} with a vague note that $T_{ex} \approx 200$ °C, based on "numerical models of mantle convection." Wyllie (1988) provided the first petrologic estimate of T_{ex} (at Hawaii) of ≈300 °C. Wyllie's calculations assumed that melting extended into the garnet stability field at Hawaii, but not beneath MORs; it is now known, however, that MORBs derive from melting at garnet–peridotite depths (Salters and Hart, 1989; MELT Seismic Team, 1998), invalidating that approach. Klein and Langmuir (1987) examined temperature variations along the global MOR systems and found differences in sub-ridge temperatures of as much as 250 °C from an analysis of crustal thickness and melt fraction, and partial melting experiments. Their analysis included MORBs from latitude 63.85–64.79 °N on the mid-Atlantic ridge, and thus encompassed the Iceland hot spot. The Klein and Langmuir (1987) estimate of 250 °C has sometimes been misunderstood to represent the thermal variations of normal MORB mantle (Anderson, 2000), however, their 250 °C range clearly represents $T^{\text{Iceland}} - T^{\text{coldest MORB}}$; it is thus neither an estimate of a MORB "thermal standard deviation", nor an estimate of excess temperature, which for Iceland would be $T^{\text{Iceland}} - T^{\text{avg. MORB}}$. Shen and Forsyth (1995) and Presnall et al. (2002) obtained smaller variations for the sub-MOR mantle, on the order of 100–140 °C. Shen and Forsyth's (1995) estimate also covered Iceland, and attempted to account for mantle heterogeneity. More recently, Asimow and Langmuir (2003) and Asimow et al. (2004) have shown how H_2O variations can diminish apparent thermal deviations in the sub-MOR mantle. Asimow et al. (2004), for example, showed that excess crustal thickness at the Azores can be explained by thermal anomalies that range from 75 °C for a dry mantle, down to 35 °C for a mantle that contains 700 ppm H_2O. Their results support, at least partly, Bonatti (1990), who suggested from his observations of abyssal peridotites, that thick crust at the Azores could be produced entirely by differences in mantle H_2O. Excluding calculations involving variable H_2O contents, most all these T estimates are based on the thickness of ocean crust, with the presumption that thick crust requires high degrees of melting, which in turn requires high temperatures. Such estimates depend upon uncertain assumptions of melt productivity during adiabatic upwelling, and the efficiency of melt extraction from the mantle. An opposing view is that thick crust indicates freezing point depression of the peridotite solidus due to the presence of volatiles (Bonatti, 1990), or the presence of more fertile mantle components (Green et al., 2001).

Albarede (1992), Herzberg and O'Hara (1998), Herzberg (2004) and Putirka (1999, 2005) have also estimated melting depths and temperatures. Their work shows that major oxide compositions are sufficiently different between MORBs and ocean-island basalts (OIBs) so as to require that at least some OIBs are derived at greater pressures and temperatures. Herzberg and O'Hara (1998) estimated excess temperatures of 100–150 °C at Iceland and 200–250 °C at Hawaii; Putirka (1999) estimated a 300 °C excess T at Hawaii (compared to the East Pacific Rise). By a similar analysis of komatiites, Herzberg (1995) further suggested that mantle excess temperatures have hovered near 200 °C since the Archean, and could have been as high as 300–400 °C for certain Archean mantle plumes. In comparison, at Iceland MacLennan et al. (2001a) obtained $T_{ex} > 200$ °C using crustal thickness and melt composition, while Ito et al. (1999) estimated $T_{ex}^{\text{Iceland}} = 180$ °C based on rheology related to partial

Table 1
Calculated parental (or mean primary) magma compositions

	Avg. MORB	Siqueiros	Iceland	Hawaii	Samoa	Kilauea-H[a]	MORB-H[a]
SiO_2	48.0	48.5	47.2	47.2	45.3	47.5	48.4
TiO_2	0.9	0.9	0.7	1.6	2.5	1.9	0.8
Al_2O_3	15.2	15.9	12.3	9.0	9.2	9.7	16.3
FeOt[b]	8.4	8.0	9.3	11.6	12.0	11.4	7.9
MnO	0.1	0.1	0.2	0.2	0.2	0.2	0.1
MgO	14.6	13.2	18.2	21.4	20.5	19.2	12.9
CaO	10.6	11.1	10.5	7.3	8.0	8.0	11.3
Na_2O	2.2	2.3	1.4	1.4	1.8	1.7	2.2
K_2O	0.0	0.0	0.1	0.2	0.7	0.4	0.0

[a] Compositions Kilauea-H and MORB-H are "representative primary magma" compositions from Herzberg (pers. comm.), for comparison. All other compositions are from this study; see Appendix A for calculation procedures).
[b] FeOt is FeO total, see Appendix A.

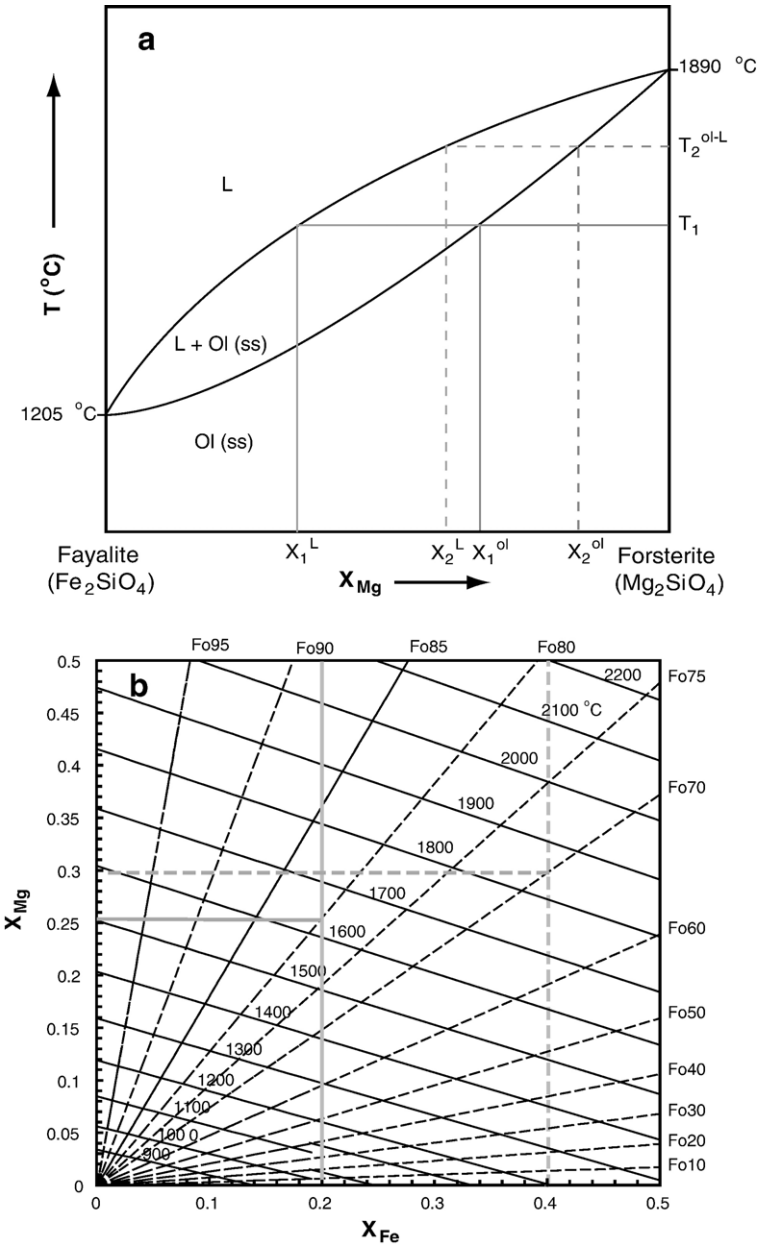

Fig. 2. The olivine binary phase diagram, (a) is compared to the Roeder and Emslie (1970) olivine thermometer for natural basaltic liquids. In the olivine binary (a), there is a monotonic relationship between temperature and the Fo content of olivine. Solid lines connect the equilibrium olivine-liquid pair X_1^{liq} and X_1^{ol}, which equilibrate at T_1. For any olivine with greater Fo content, such as X_2^{ol}, it will equilibrate with a liquid with higher MgO content, X_2^{liq}, at a higher T, T_2 (connected by dashed lines). But natural liquids do not have an olivine stoichiometry, and the monotonic relationship between Fo and T does not apply. (b) Shows the graphical olivine-liquid thermometer of Roeder and Emslie (1970) (their Fig. 7). The near-horizontal lines are isotherms, shown in °C, and calculated from Eq. (1), and models A and B from Putirka (2005). Lines that radiate from the origin are lines of constant Fo content, as determined by the Fe–Mg exchange coefficient, $K_D(Fe–Mg)^{ol\text{-}liq}=(X_{Mg}^{liq}X_{Fe}^{ol})/(X_{Mg}^{liq}X_{Fe}^{ol})$, which is 0.32 in (b). If both X_{Fe}^{liq} and X_{Mg}^{liq} are known, the intersection of those compositions will yield the temperature at which olivine will become saturated (from the isotherms), and the composition of that olivine (from the radiating lines of constant Fo). But one need not use X_{Mg}^{liq} as input, and the effect of X_{Fe}^{liq} is very important: Notice that if a liquid is known to have $X_{Fe}^{liq}=0.4$, and it is known to have equilibrated with an olivine of Fo 70, the equilibration T would be ≈1840 °C; in contrast, if a different liquid has $X_{Fe}^{liq}=0.2$, and is known to have equilibrated with an olivine of Fo 80, the equilibration T would be much lower, ≈1630 °C, even the though the Fo content of the equilibrated olivine is greater. It should also be noted that in the latter technique, X_{Mg}^{liq} for the liquid can be retrieved when FeO^{liq} and Fo are known.

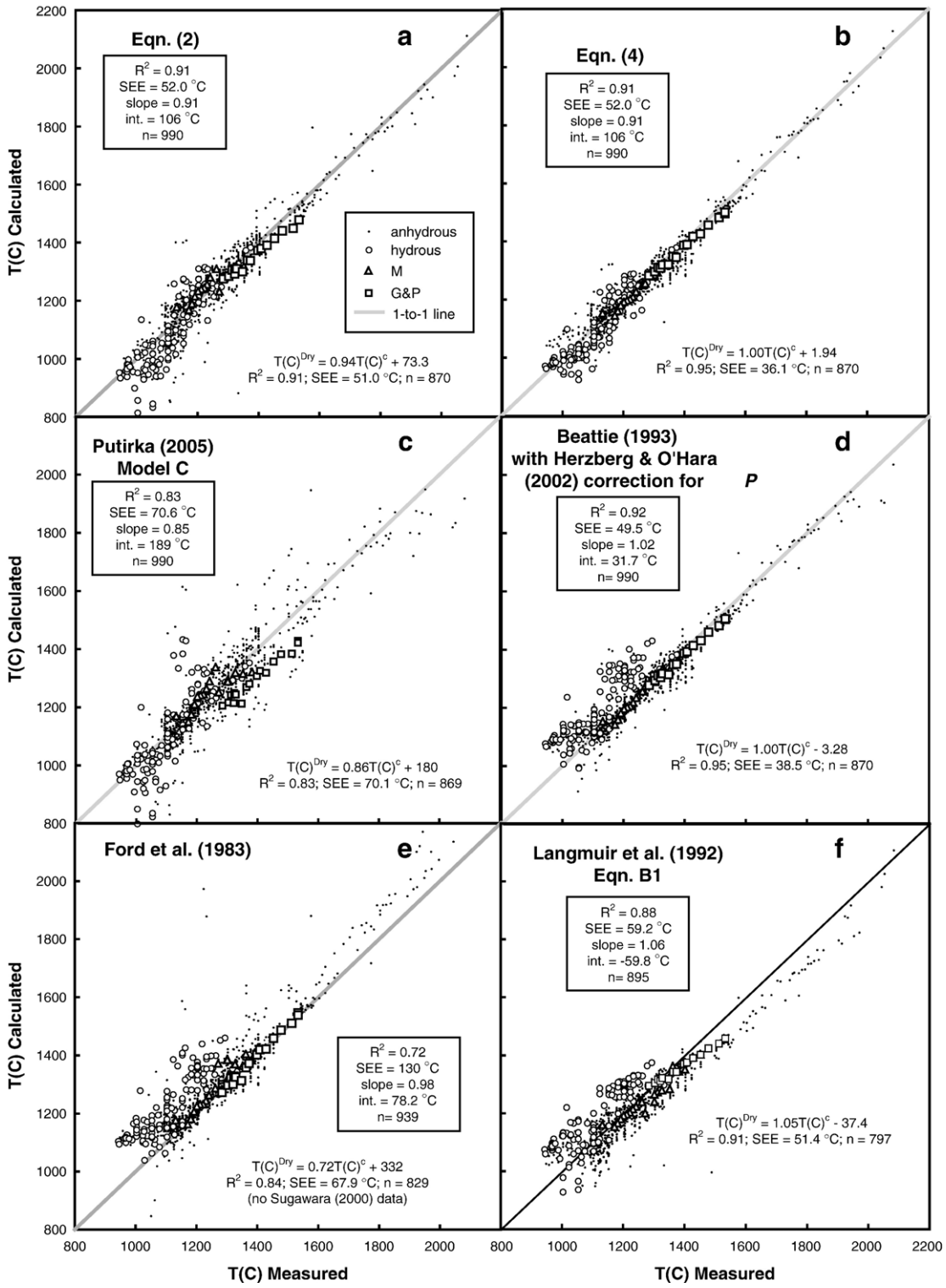

melting. Though temperatures were not quantified, Fram and Lesher's (1997) analysis of melting depths related to the Iceland melting anomaly implies comparable temperature differences. More recently, Putirka (2005) used olivine thermometry to calculate $T_{ex} \approx 220$ °C at Hawaii and ≈ 170 °C at Iceland.

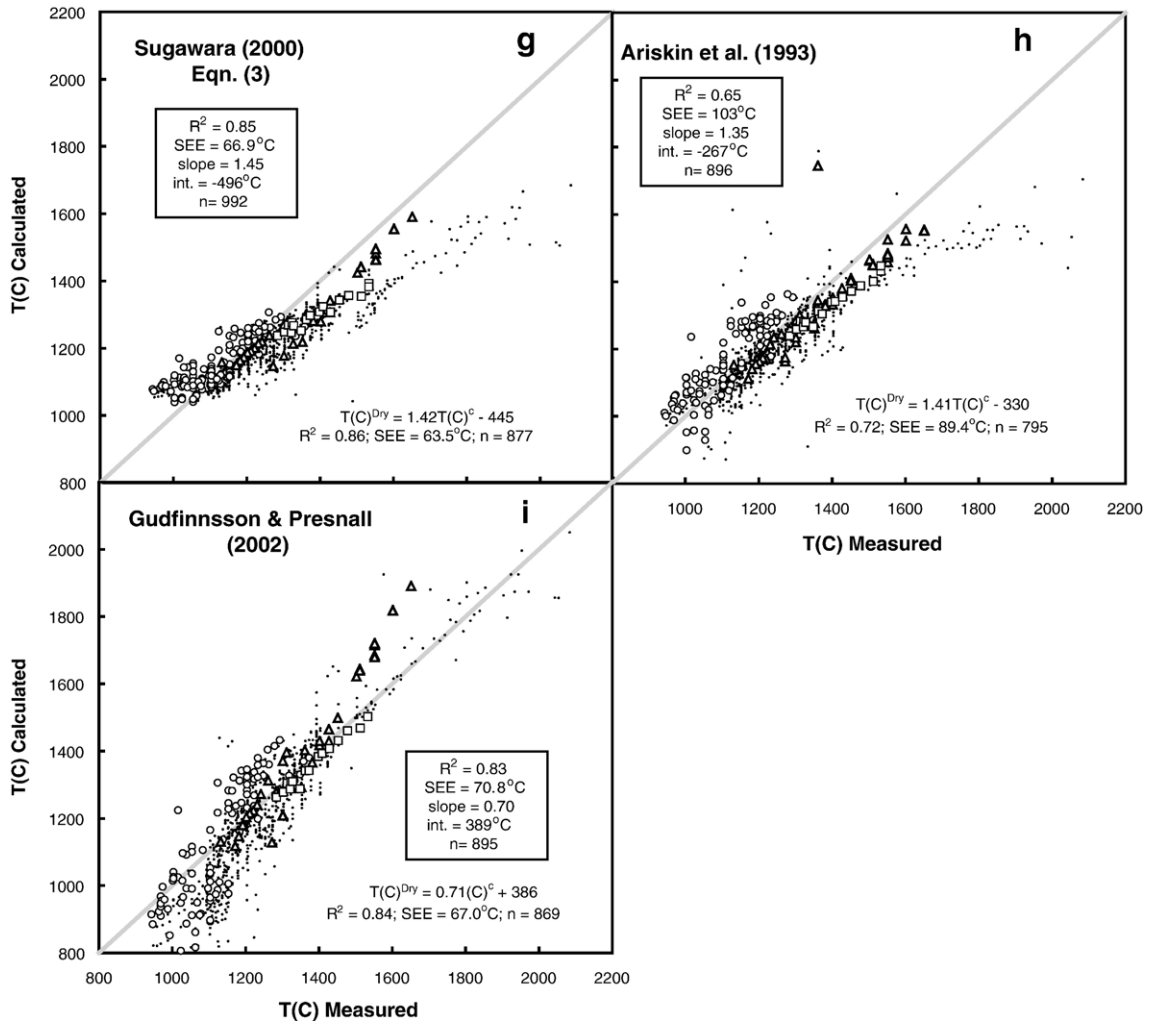

Fig. 3. (a) Eq. (2), (b) Eq. (4), and (c)–(i) other published expressions of $D_{Mg}^{ol/liq}=f(T)$, are tested for their ability to recover T for olivine-saturated partial melting experiments. A one-to-one line is shown in each panel. G&F are data from Gudfinnsson and Presnall (2000); M are data from Montierth et al. (2000). R^2 values, the standard errors of estimate (SEE), and slope and intercept values for the regression equation $T(C)^{measured}=mT(C)^{calculated}+b$ are given for regression lines. Systematic error is indicated by slope and intercept values that deviate from 1 and 0 respectively. The equations $T(C)^{Dry}=mT(C)^{c}+b$ compare slope and intercept values for anhydrous experiments only; $T(C)^{Dry}$ and $T(C)^{c}$ are respectively the reported experimental and calculated values. 1007 experiments were used for testing and calibrations, from the following studies (experiments from LDEO are corrected for the calibration effects as noted in Longhi, 2005): Baker and Eggler (1987), Baker et al. (1994), Baker and Stolper (1994), Baker et al. (1995), Bartels et al. (1991), Blatter and Carmichael (2001), Dalton and Presnall (1998a,b), Draper and Johnston (1992), Dunn and Sen (1994), Elthon and Scarfe (1984), Esperança and Holloway (1987), Falloon and Green (1987), Falloon et al. (1988), Falloon et al. (1997), Falloon et al. (2001), Fram and Longhi (1992), Gaetani and Grove (1998), Gee and Sack (1988), Grove et al. (1990), Grove et al. (1992), Grove et al. (1997), Grove et al. (2003), Grove and Juster (1989), Gudfinnsson and Presnall (2000), Herzberg and Zhang (1996), Juster et al. (1989), Kinzler and Grove (1985), Kinzler and Grove (1992a), Kogiso et al. (1998), Kogiso and Hirschmann (2001), Longhi (2002), Longhi and Pan (1988), Longhi et al. (1978), Longhi et al. (1999), Montierth et al. (2000), Moore and Carmichael (1998), Müntener et al. (2001), Murck and Campbell (1986), Parman et al. (1997), Pichavant et al. (2002), Righter and Carmichael (1996), Robinson et al. (1998), Sack et al. (1987), Schwab and Johnston (2001), Sisson and Grove (1993a,b), Sugawara (2001), Takagi et al. (2005), Thy (1991), Tormey et al. (1987), Trönnes et al. (1992), Vander Auwera and Longhi (1994), Vander Auwera et al. (1998), Wagner and Grove (1997), Walker et al. (1979), Walter (1998), Wasylenki et al. (2003), Xirouchakis et al. (2001), Yang et al. (1996).

Petrologic estimates of T_{ex} are consistent with temperatures inferred from "excess topography", i.e., the shallow bathymetry and uplift exhibited at oceanic hot spots. For instance, although Sleep (1990) admitted that excess temperatures are "not tightly constrained by geophysical considerations", he applied $T_{ex}=200$ °C at Hawaii and Iceland to explain their topographic expressions. Similarly, Schilling (1991) calculated excess

temperatures for 13 different hot spots, that range from 160 °C (Tristan) to 280 °C (Circe), and Watson and McKenzie (1991) used a combination of excess topography, geoid height and melt productivity, to derive a T_{ex} at Hawaii of 278 °C. Ribe and Christensen (1999) expanded upon the Watson and McKenzie approach to arrive at $T_{ex} \approx 160$ °C at Hawaii.

2.3. Some contrasting viewpoints and maximum temperatures

The weight of dynamic and petrologic T estimates indicates that the highest mantle temperatures are at hot spots, with values of T_{ex} between 160–300 °C. However, except for Putirka (2005), and Albarede (1992), errors are not well quantified. In addition, Green et al. (2001) present a serious challenge to this tide of work. They observe that maximum forsterite contents (Mg_2SiO_4; Fo = Mg#$^{ol} = X^{ol}_{Mg}/(X^{ol}_{Mg}+X^{ol}_{Fe})$, where X^{α}_{i} are cation fractions of i in phase α) of olivine phenocrysts at MORs match or exceed those found at Hawaii, and conclude that $T_p \approx 1430$ °C, at both Hawaii and at MORs. Their strategy of examining Fo_{max} is significant. It is well established that temperatures decrease dramatically along liquid lines of descent (O'Hara, 1978), and that any viable model for generation of a primitive liquid requires equilibration of that liquid with mantle olivine (O'Hara, 1968, 1970). R.N. Thompson (1978) was perhaps the first to recognize that olivine phenocrysts in MORB range to Fo91, and that temperature estimates that implicate lower Fo contents likely underestimate mantle temperatures. Green et al.'s (2001) use of Fo_{max} for MORB phenocrysts is thus a valid attempt to measure the maximum temperatures in the sub-MOR mantle. Anderson (2000) also provides a challenge to the plume model. He argues that 1) there are no thermally undisturbed regions of the upper mantle (isotherms in the uppermost mantle are unlikely to be flat), 2) horizontal temperature variations exceed 200 °C at shallow depths, and 3) absolute temperatures encompass estimates of plume temperatures. In this view, T_{ex}'s as great as 200–250 °C do not require a source of excess heat at depth; though there are problems with the Anderson (2000) analysis (see Section 4.), we must understand sub-ridge temperature variations to estimate T_{ex}.

To address these issues we test new and published olivine-liquid thermometers, and examine global variations in FeO^{liq} among MORBs to assess the mean and standard deviation of sub-MOR temperatures. These results lead to our proposal for a new convective geotherm, which we compare to other appraisals of upper mantle temperatures. We then calculate T_{ex} at Hawaii, Samoa and Iceland.

3. Olivine thermometry

Because primitive oceanic basalts equilibrate with olivine in their source region (O'Hara, 1968), mantle temperatures can be estimated from olivine-liquid equilibria, provided that one can reconstruct coexisting primitive liquid and olivine compositions. Olivine thermometry provides a test that is independent of temperature estimates that derive from crustal thickness and has greater precision. To estimate temperatures we require 1) the FeO^{liq} (literally, Fe as Fe^{2+}) of mantle-equilibrated liquids, or an FeO–MgO trend-line along which liquids are olivine saturated (see Appendix A, for calculations regarding FeO), 2) the Fo_{max} of olivines that equilibrate with parental liquid compositions, 3) the value for the Fe–Mg exchange coefficient between olivine and liquid, $K_D(Fe–Mg)^{ol\text{-}liq}$, and estimates of 4) the pressure (P) of olivine-liquid equilibration, and 5) fO_2 conditions. Temperature can be calculated from these five variables alone, if one applies the composition independent thermometers of Putirka (2005). To estimate T more precisely we estimate MgO^{liq} for parental liquids (using FeO^{liq}, $K_D(Fe–Mg)^{ol\text{-}liq}$ and Fo_{max} as input; see Appendix A) and then reconstruct the SiO_2^{liq} and $Na_2O^{liq}+K_2O^{liq}$ for parental liquids to use as input into geothermometers (Table 1).

It is well established that $D^{ol/liq}_{Mg} = f(T)$ and that coexisting olivine-liquid pairs that exhibit low $D^{ol/liq}_{Mg} (= X^{ol}_{Mg}/X^{liq}_{Mg}$, where X_{Mg} is the cation fraction of Mg in olivine or liquid) have high melting temperatures (e.g., Roeder and Emslie, 1970; Sugawara, 2000; Putirka, 2005). The olivine binary phase diagram (Fig. 2a) shows that high Fo contents require equilibrium with liquids that have high Mg# (Mg#$^{liq} = X^{liq}_{Mg}/(X^{liq}_{Mg}+X^{liq}_{Fe})$, with Fe as Fe^{2+}). In the olivine binary, there is a monotonic relationship between Fo content and T (and Mg#^{liq}) (Fig. 2). In natural silicate liquids, though, Fe and Mg can vary independently, and the monotonic relationship between T and Fo content no longer applies. The Mg# of a liquid will still dictate the Mg# (i.e., Fo content) of a coexisting olivine, depending upon the value of the Fe^{2+}–Mg exchange coefficient, $K_D(Fe–Mg)^{ol\text{-}liq} = (X^{liq}_{Mg} X^{ol}_{Fe})/(X^{liq}_{Mg} X^{ol}_{Fe})$, (Roeder and Emslie, 1970; Herzberg and O'Hara, 1998; Toplis, 2005). But if a liquid has low Fe^{2+}, then even at a high Mg#, it will have low MgO^{liq}, and hence high $D^{ol/liq}_{Mg}$, and olivine-liquid equilibration will occur at low T. Similarly, if a liquid has high Fe^{2+}, then high

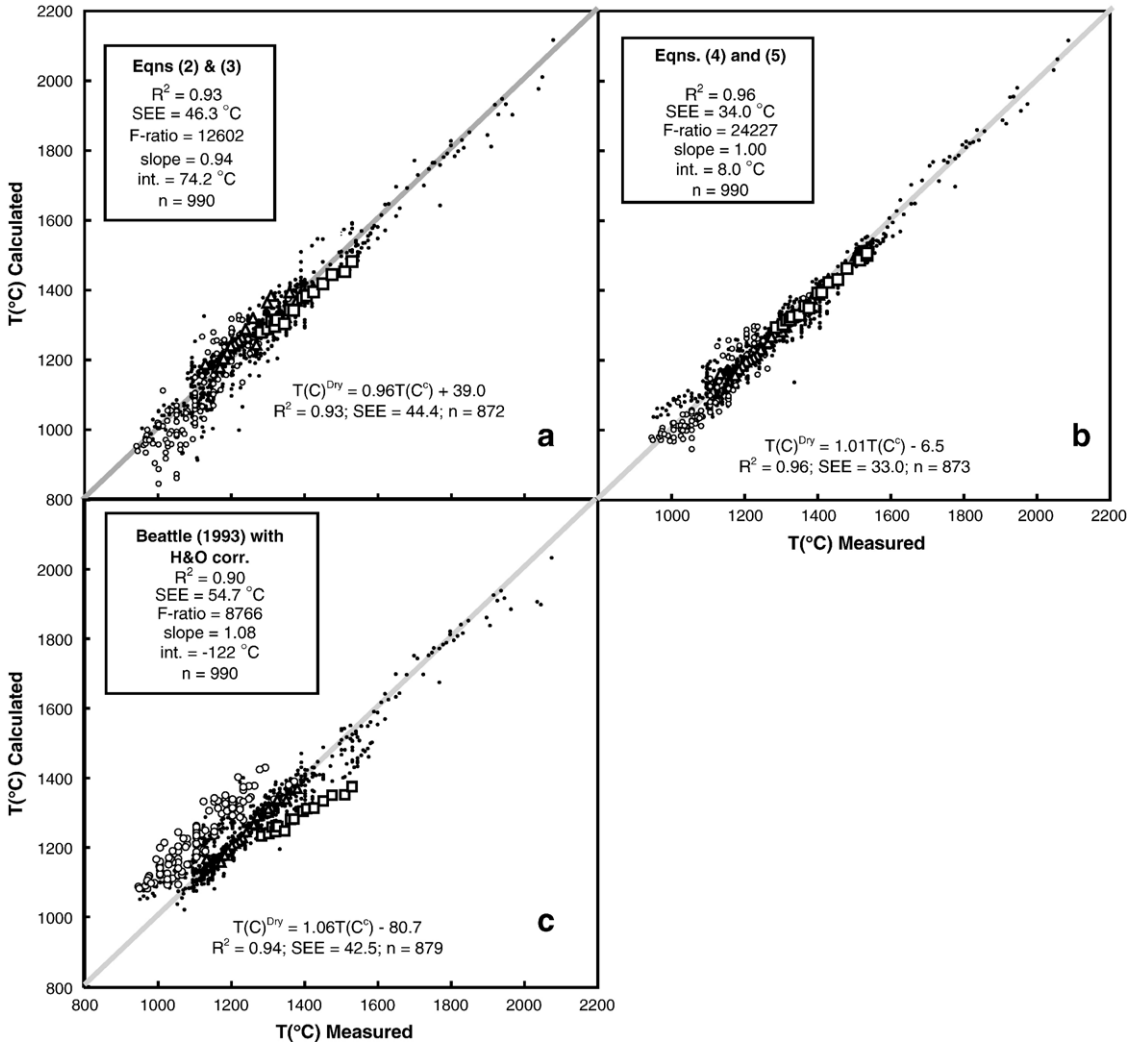

Fig. 4. Temperatures are calculated for experimental data using Eq. (1) in combination with (a) Eqs. (2) and (3), (b) Eqs. (4) and (5) and (c) Eq. (10) from Beattie (1993; using coefficients for Fe and Mg partitioning, and pressure corrections from Herzberg and O'Hara, 2002). Statistics and data are as in Fig. 3.

Mg# implies high MgO^{liq}, and therefore low $D_{Mg}^{ol/liq}$, and high equilibration *T*. This insight is not new, and is implicit in the Roeder and Emslie (1970) olivine thermometer (Fig. 2b; their Fig. 7).

3.1. Thermodynamic basis for olivine thermometry

Since most basalts have had their MgO contents affected by olivine fractionation, primitive MgO^{liq} contents are commonly estimated by determining the MgO content of a liquid that would be in equilibrium with a high Fo (mantle) olivine, usually taken as Fo90–92 (Albarede, 1992; Kelemen et al., 1997; Green et al., 2001). The quantity $D_{Mg}^{ol/liq}$ is then calculated by pairing the model primitive liquid with the assumed olivine composition and *T* is calculated from $D_{Mg}^{ol/liq} = f(T)$. Estimates of MgO^{liq} provide the principal sources of error. However, since FeO^{liq} remains nearly constant during olivine fractionation (Langmuir and Hanson, 1980; Klein and Langmuir, 1987; Putirka, 2005), an alternative strategy is to use FeO^{liq} (as derived from so called olivine control lines (Powers, 1955), where olivine addition/removal controls whole rock composition) for *T* estimation, and MgO^{liq} becomes output, rather than input (Appendix A).

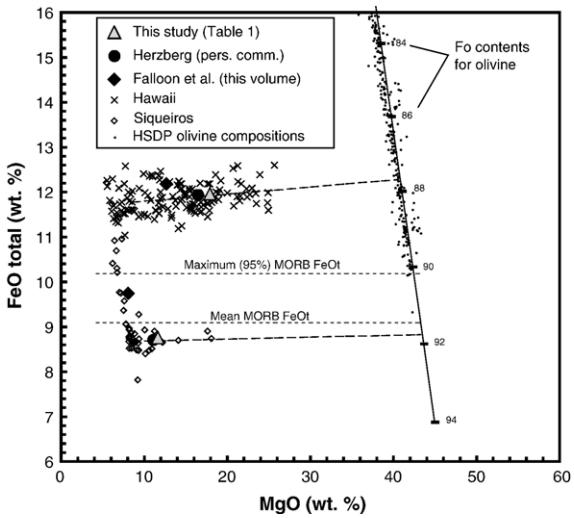

Fig. 5. FeOt–MgO variation diagram for Hawaii and Siqueiros, and a comparison of calculated primary/parental magma compositions from this study and Herzberg (pers comm.) (Table 1), and Falloon et al. (this volume). Hawaii data are from Rhodes and Vollinger (2004) and Norman and Garcia (1999); Siqueiros data are from Perfit et al. (1996). Regression lines (dashed) through high MgO "olivine control" lines (i.e., variation diagrams where olivine addition/subtraction controls bulk composition) have slopes that are effectively flat (slope=0.015 at Hawaii and 0.004 at Siqueiros). Horizontal curves illustrate mean and maximum FeOt values for MORB (see Fig. 7). Also plotted is a model curve (solid curve) for olivine compositions (black dots) that range from Fo84-95, with natural olivine compositions from HSDP samples. The parental/primary magma compositions of this study and Herzberg are clearly very close, though our compositions have slightly greater MgO than Herzberg's preferred compositions. The compositions of Falloon et al. have FeOt that is slightly too high at Hawaii, and much too high for MORB, the latter approaching the maximum FeOt for MORB. These compositional differences, more so than differences in thermometers, drive much of the differences in estimates of olivine equilibration, mantle potential, and mantle excess temperatures.

The Roeder and Emslie (1970) approach to olivine thermometry provides an elegant graphical means to assess error, and supports the use of different input (Putirka, 2005). In this approach, temperatures are calculated using the following expression:

$$[X_{Mg}^{liq}][D_{Mg}^{ol/liq}] + [X_{Fe}^{liq}][D_{Fe}^{ol/liq}] = 0.667 \quad (1)$$

In (Eq. (1)), X_{Mg}^{liq} and X_{Fe}^{liq} are the cation fractions of Mg and Fe^{2+} in the liquid and $D_{Mg}^{ol/liq}$ and $D_{Fe}^{ol/liq}$ are the respective partition coefficients, X_{Mg}^{ol}/X_{Mg}^{liq} and X_{Fe}^{ol}/X_{Fe}^{liq}. Temperature sensitive expressions for $D_{Mg}^{ol/liq}$ and $D_{Fe}^{ol/liq}$ (Eqs. (2) and (3) below) are substituted into Eq. (1), and T is varied until the sum of the expression yields the cation fraction of Mg+Fe in olivine ($(Mg,Fe)_2SiO_4$), i.e., 2/3 (see Langmuir and Hanson, 1981; Putirka, 2005).

Putirka (2005) calibrated P-independent olivine-liquid equilibria to show that high FeO^{liq} at Hawaii and Iceland require higher equilibration temperatures compared to MORs (220 °C and 170 °C respectively), even though Fo_{max} is similar at MORs, Iceland and Hawaii. To refine these estimates, new P-sensitive $D^{ol/liq}$ is calibrated and tested using 993 experimental observations of olivine-liquid equilibrium. Eqs. (2)–(5) were calibrated using 137 experimental data (selected from Falloon and Green, 1987; Falloon et al., 1988; Trönnes et al., 1992; Sisson and Grove, 1993a, b; Yang et al., 1996; Grove et al., 1997; Parman et al., 1997; Wagner and Grove, 1997; Kogiso et al., 1998; Walter, 1998; Montierth et al., 2000; Falloon et al., 2001; Gudfinnsson and Presnall, 2000; Longhi, 2002). The remaining 856 experimental data (Fig. 3) were used for test purposes; the test data encompass the pressure range 0.0001–15.5 GPa and the temperature range 965–2080 °C. Each independent variable has a high F-ratio and was tested using leverage plots to ensure significance:

$$\ln D_{Mg}^{ol/liq} = -2.158 + 55.09\frac{P(GPa)}{T(°C)} - 6.213 \times 10^{-2}[H_2O^{liq}] + \frac{4430}{T(°C)} + 5.115 \times 10^{-2}[Na_2O^{liq} + K_2O^{liq}] \quad (2)$$

$$\ln D_{Fe}^{ol/liq} = -3.300 + 47.57\frac{P(GPa)}{T(°C)} - 5.192 \times 10^{-2}[H_2O^{liq}] + \frac{3344}{T(°C)} + 5.595 \times 10^{-2}[Na_2O^{liq} + K_2O^{liq}] + 1.633 \times 10^{-2}[SiO_2^{liq}] \quad (3)$$

In Eqs. (2) and (3), T is in °C and P is in GPa; terms such as SiO_2^{liq}, represent the weight % of the indicated oxide in the liquid phase, while $D_{Mg}^{ol\text{-}liq}$ refers to the cation fraction ratio of Mg between olivine and liquid. For test data, we make use of post-1987 1 atm data, because of the development of techniques to minimize alkali loss in open furnace systems (e.g. Tormey et al., 1987).

As we will show, the Beattie (1993) thermometer is remarkably accurate, and so we re-calibrate his Eq. (10), adding a term for water, and additional, thermodynamically derived terms (Putirka, 1998, Eq. (7)) for P:

$$T(°C) = \frac{15294.6 + 1318.8P(GPa) + 2.4834[P(GPa)]^2}{8.048 + 2.8532\ln D_{Mg}^{ol/liq} + 2.097\ln[1.5(C_{NM}^{L})] + 2.575\ln[3(C_{SiO_2}^{L})] - 1.41NF + 0.222H_2O + 0.5P(GPa)} \quad (4)$$

$$T(°C) = \frac{461.29 + 84.9P(GPa) + 0.588[P(GPa)]^2}{0.355 + 0.06986\ln D_{Fe}^{ol/liq} - 0.00435\ln[1.5(C_{NM}^{L})] - 0.0523\ln[3(C_{SiO_2}^{L})] - 0.0217NF + 0.000893H_2O + 0.04P(GPa)} \quad (5)$$

Because calibration of Eqs. (4) and (5) involves non-linear regression methods, F-tests are not possible and the coefficients derive from regression of all 993 experimental data. We apply the activity models of Beattie (1993), but for simplicity, H_2O is expressed in wt.%. In these expressions, $C_{NM}^{liq} = X_{Mg}^{liq} + X_{Fe2+}^{liq} + X_{Ca}^{liq} + X_{Mn}^{liq}$; $C_{SiO2}^{liq} = X_{Si}^{liq}$; $NF = 7/2\ln(1 - X_{Al}^{liq}) + 7\ln(1 - X_{Ti}^{liq})$, where X_i^{liq} is the cation fraction of element i in the liquid phase (see Beattie, 1993).

We use these equations with estimates of Fo_{max}, the maximum Fo content of olivines with which parental liquids (Table 1) may have equilibrated. We cannot demonstrate that primitive liquids have not equilibrated with olivines with higher Fo contents, but below we show (Section 4) that values of $Fo_{max} \approx 91.5$ are generally consistent with an approach to mantle values. If nothing else, our temperatures are minimum estimates. Herzberg and O'Hara (2002) have suggested that fractional melting may pose difficulties with the interpretation of high Fo olivines. But we emphasize that fractional melting still implies equilibrium; provided an equilibrium FeO^{liq} can be identified, it matters little whether melts were whisked away by a batch or fractional process. A more serious concern is whether any particular olivine composition has had its composition set by sub-solidus equilibration.

3.2. Tests of new and existing models

Fig. 3 illustrates tests of a number of published olivine-liquid thermometers that utilize X_{Mg}^{ol} and X_{Mg}^{liq} as input (Ford et al., 1983; Langmuir et al., 1992; Ariskin et al., 1993; Beattie, 1993; Sugawara, 2000; Gudfinnsson and Presnall, 2001; Putirka, 2005). For dry conditions at low T, the model of Beattie (1993) (using the pressure correction of Herzberg and O'Hara (2002)), is clearly the most accurate of any published model; but comparison of one-to-one correlation lines, and slopes and intercepts of regression lines through T(°C) calculated vs. T(°C) measured shows that Eqs. (2) and (4) exhibit the least error. When water contents are low, however, it would not be unwarranted to average T estimates from Eqs. (2)–(4) and Beattie (1993).

In contrast to the use of $D_{Mg}^{ol/liq}$ alone, isotherms in the Roeder and Emslie (1970)-type diagram are calculated using Eq. (1), and equations such as $D_{Mg}^{ol/liq} = f(T)$ and $D_{Fe}^{ol/liq} = f(T)$ simultaneously (see Langmuir and Hanson, 1981; Putirka, 2005). This approach does not necessarily require X_{Mg}^{liq} as input. We test the precision with which such isotherms can be calculated, using Eqs. (2)–(5), Putirka (2005), Ford et al. (1983) and the Beattie (1993) (as throughout this paper, using the Herzberg and O'Hara (2002) pressure correction) models (Fig. 4). As might be expected, models that exhibit systematic error in their individual D's (Fig. 3), retain their systematic error (Fig. 4), as is evident in the F-ratios, and slope and intercept values (Fig. 4); Eqs. (2)–(5) nearly eliminate this systematic error.

In Appendix A, we compare T estimates for model MORB, Iceland, Samoa and Hawaiian parental liquid compositions, as calculated by us (Table 1; see Appendix A) and by Herzberg (pers. comm.). These tests (Table A1) show that, provided one is consistent about the choice of input parameters, T estimates from various models differ by as little as 27 °C (for MORB), with standard deviations that are within 1σ model error. The large differences between our mantle potential temperatures, and T estimates of, say, Falloon et al. (this volume), depend as much or more upon the derived or implicit bulk compositions and olivine Fo contents (Fig. 5; see Appendices A and B)). In some cases, though, temperature estimates diverge by more than 100 °C for equivalent input (Table A2), in which case predicted values for Fo and $K_D(Fe–Mg)^{ol\text{-}liq}$ may be used to decide which thermometers yield the best estimates (Appendix A).

4. Ambient mantle temperatures

As noted, Anderson (2000) presents an interesting challenge to the mantle plume model, proposing that the apparent sites of "excess heat" (e.g., Hawaii, Iceland) reflect temperature variations in the uppermost mantle rather than from deeper thermal inputs. The source of Anderson's (2000) proposed 200 °C+ thermal variance is unfortunately vague. Some studies cited by Anderson (2000) estimate T variations that can in fact be viewed as supportive of the plume model (e.g., Klein and Langmuir, 1987; Schilling, 1991; see Section 2.2). In addition, seismically detected long-wavelength T variations are not only thermally imprecise, but are unlikely to capture hot narrow upwellings. It is also unclear to what extent the seismic long-wavelength T estimates cited by Anderson (2000) were filtered for the effects of cold subducted slabs, or lithosphere roots, whose thermal structures are irrelevant to the temperature ranges that drive intra-plate volcanism. However, Anderson (2000) raises a fundamental question: is the variation of temperatures beneath MORs so great so as to encompass intra-plate estimates of T_{ex}? If MORB derive from regions of the mantle with greater than 200 °C variations in T, especially in the absence of a hot spot influence, then excess temperatures of a similar magnitude at mid-plate settings need not be interpreted as deep-seated thermal plumes. A quantitative estimate of the range of sub-MOR mantle temperatures is thus required.

Mid-ocean ridge basalts result from passive mantle upwelling (see McKenzie and Bickle (1988) for a summary of the decisive arguments), and thus provide a global sampling of the upper mantle, absent the influence of putative mantle plumes. To measure the mean, range and standard deviation of upper mantle temperatures, we use a global database of 22,591 MORBs and 2,845 MORB-derived olivines (PETDB: http://www.petdb.org/), including samples from the Siqueiros Transform (Perfit et al., 1996). The Siqueiros samples are important because Siqueiros is the only MOR location where liquids can be traced to an olivine-only fractionation line ("olivine control"). These data allow a direct estimate of primitive FeO^{liq} contents, and the olivines that coexisted with such liquids (Fig. 6a). The global MORB database is used to examine the global range in FeO^{liq} (Fig. 7), which reflects the T range in the sub-MOR mantle; though Iceland proper is excluded from this MORB data set, there is no additional filtering of this database for the effects of hot spot-influenced ridge segments.

4.1. FeO in primitive MORB liquids

For consistency, we first convert all analyses of Fe to FeO total (FeOt; see Appendix A), and calculate FeO (Fe as Fe^{2+}) assuming the fO_2 conditions of Bezos and Humler (2005) and by use of the models of Kress and Carmichael (1988) (see Appendix A). Where we note FeO or FeO^{liq} (as opposed to FeOt) we always mean $Fe^{2+}O$, and all temperatures that require Fe as input use FeO^{liq}. An inflection in the global MORB database, at approximately 9.5 wt.% MgO, shows the transition from "olivine control" (fractionation of olivine alone) at high MgO, to the co-precipitation of olivine and plagioclase (lower MgO), at least for high Fe primitive liquids. An orthogonal regression line is shown for MORB with MgO < 9.5 wt.%, that describes the olivine + plagioclase fractionation trend. The horizontal lines at 7 and 9.6 wt.% $FeOt^{liq}$ represent the upper and lower limits for primitive $FeOt^{liq}$ in MORB that can generate 95% of MORB compositions through olivine fractionation, followed by olivine + plagioclase fractionation at MgO ≤ 9.5 wt.%. Provided that primitive MORB equilibrate with olivine, these upper and lower bounds on $FeOt^{liq}$ must reflect variations in T for the sub-MOR mantle, even if the mantle is heterogeneous with respect to Fe (Shen and Forsyth, 1995); olivine-liquid thermometers, though, by their calibration, account for such variations, and so are independent of the composition of the mantle source (only estimates of melt fraction, F, depend upon a model for mantle composition; Appendix A).

4.2. Maximum Fo in MORB olivines

To estimate temperature, we must estimate the value for the maximum Fo content of olivines equilibrated with MORB. To estimate Fo_{max} for MORBs we compare Fo and CaO contents of olivines from the ocean basins (Fig. 8a). We include data from abyssal hills, seamounts, fossil spreading ridges, transform fault zones, as well as spreading ridges; the data are filtered so that divalent cation sums in olivine, calculated on a 4-oxygen basis, are between 2.99–3.01. Olivines from ultramafic rocks can be discerned from phenocryst olivines in that their CaO contents are much lower (<0.17 wt.%) than those of phenocrysts in lavas (Norman and Garcia, 1999). Low CaO is accompanied by high NiO, and undoubtedly reflects depletion of a solid residue in CaO due to melt removal. Phenocryst Fo_{max} values also overlap with Fo contents from ultramafic olivines. We cannot exclude the possibility that ultramafic olivines have re-equilibrated at subsolidus conditions, but the cluster of ultramafic

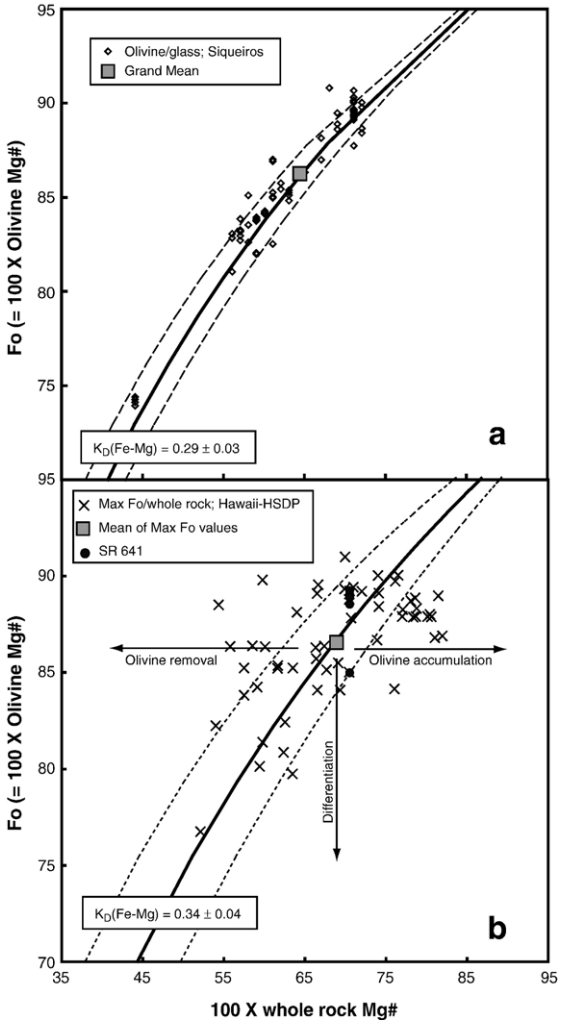

Fig. 6. (a) Siqueiros glass and coexisting olivine compositions are consistent with an Fe–Mg exchange coefficient, $K_D(\text{Fe–Mg})^{\text{ol-liq}} = (X^{\text{liq}}_{\text{Mg}} X^{\text{ol}}_{\text{Fe}})/(X^{\text{liq}}_{\text{Mg}} X^{\text{ol}}_{\text{Fe}})$, of 0.29 (Hays et al., 2004 and new data). (b) Maximum Fo contents from HSDP (Hawaii Scientific Drilling Project) lavas (this study) are compared to HSDP whole rock compositions (Rhodes and Vollinger, 2004); their mean composition suggests equilibration at $K_D(\text{Fe–Mg})^{\text{ol-liq}} = 0.34$. Olivines from sample SR641 (18.33% MgO) all lie within the ±0.03 window for $K_D(\text{Fe–Mg})^{\text{ol-liq}}$ suggesting that this HSDP sample might closely approach a parental magma composition. Arrows show the directions in which whole-rock-Fo_{max} pairs will be driven, for olivine accumulation, removal, or differentiation. It is not necessary that the mean value reflects the true $K_D(\text{Fe–Mg})^{\text{ol-liq}}$, but if the mean does not reflect equilibrium in this instance, a mass balance problem ensues: high-density olivine-laden slurries must then be preferentially erupted over low density, olivine-depleted liquids. This seems unlikely, and also unnecessary, given that experimental studies suggest that $K_D(\text{Fe–Mg})^{\text{ol-liq}}$ increases with increased P (Herzberg and O'Hara, 1998; Putirka, 2005) (see Appendix for discussion of fO_2 and calculation of Fe^{3+}/Fe^{2+} ratios).

olivines in Fig. 8a has a mean and maximum for Fo of 90.2 and 91.6 respectively, which overlaps with the maximum values obtained from phenocrysts. This overlap occurs in the range that has been inferred to represent mantle olivine compositions (Fo90–92; Albarede, 1992), and indicates that phenocryst Fo_{max} values in all likelihood approach mantle-equilibrated compositions. For temperature estimation, we use Fo = 91.5, as this value appears representative of Fo_{max} for global MORB. One caveat regarding PETDB MORB olivines is required: 81% (21) of all olivines with Fo > 91 and 100% (6) with Fo > 91.5 derive from a single study (Eissen, 1982), which comprises 19% (555) of the database. If the Eissen (1982) data are excluded, Fo_{max} of the remaining 2290 olivines is 91.3. The Eissen (1982) subset is thus suspected to have some analytical bias. It should be noted that olivines with Fo ≈ 91.9 do not derive from samples with the highest FeO, and hence maximum MOR temperature estimates are unaffected. Fig. 8a suggests that Fo_{max} is unlikely to range much higher than 91.6 for most MORBs.

Interestingly, our results (below) suggest an explanation for the non-Gaussian distribution of olivine phenocrysts, i.e., the sharp drop in numbers of phenocrysts at high Fo (Fig. 8b). We propose that the mantle geotherm, perhaps aided by a mantle that is approximately homogenous in its major element content, provides a natural upper limit to olivine Fo contents during partial melting.

4.3. Ambient mantle temperature estimates

Fig. 9a shows olivine-equilibration and mantle potential temperatures for Siqueiros and global MORB (Fig. 7). $K_D(\text{Fe–Mg})^{\text{ol-liq}}$ is calculated to be 0.31 (see Appendix A). At Siqueiros, we derive an olivine-liquid equilibration temperature of 1380 °C at 0.8 GPa; the mean FeO for MORB is greater than at Siqueiros, and so at 0.8 GPa yields an olivine-equilibration temperature of 1405 °C. Our method of temperature estimation implies a value for parental MORB MgO^{liq}; a complete reconstruction for a MORB parental liquid is given in Table 1 (see Appendix A),

We convert these temperatures to mantle potential temperatures, T_p (Fig. 1; Appendix A). To calculate $T^{\text{ol-liq}}$ and T_p, we assume a depth of equilibration of 0.8 GPa, which is at the shallow end of the range of partial melting depths estimated by Kinzler and Grove (1992b) and somewhat more shallow than the 1.15 GPa used for the T_p calculation by Putirka (2005). In regard to T_p, the global MORB FeOt range (7 wt.% ≤ FeOt ≤ 9.6 wt.%) translates to a range in T_p of 140 °C (excluding Iceland). Siqueiros

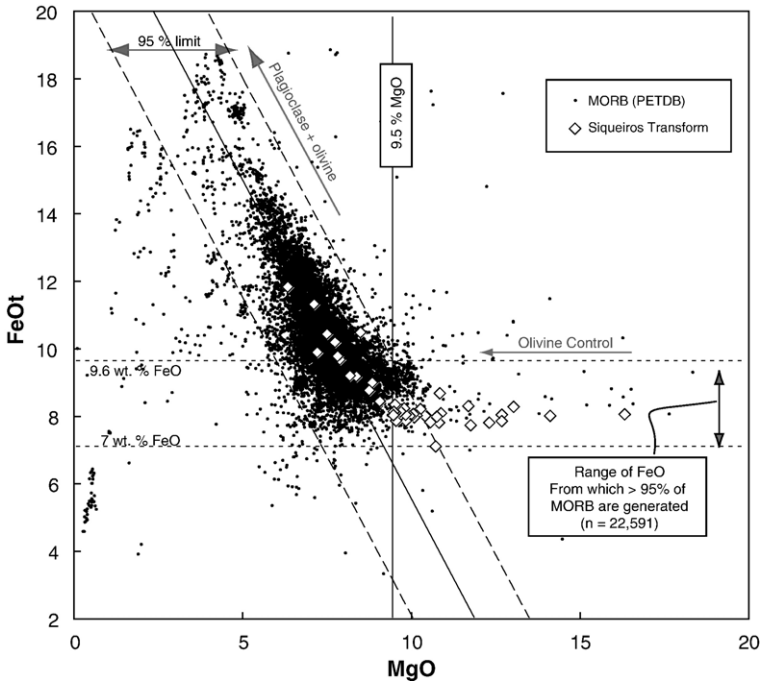

Fig. 7. PETDB (glass and whole rocks) is used to determine global variations in $FeOt^{liq}$ for MORBs. The negative trend exhibited by the majority of data have compositions controlled by olivine+plagioclase fractionation. An orthogonal regression line is shown for MORBs with <9.5 wt.% MgO, which is used to define the slopes of the two parallel lines, which encompass 95% of MORBs. Horizontal lines at $FeOt^{liq}$=7 and 9.6 wt.% indicate the range of primitive $FeOt^{liq}$ contents that can explain 95% of MORB FeO variations through olivine, followed by olivine+plagioclase fractionation. The noted range of FeO^{liq} contents can be use to bracket the range of temperatures that characterize the sub-MOR mantle.

samples lie near the middle of this range with T_p=1441 °C, but just below the T_p derived using global mean MORB FeO, which yields T_p=1466 °C. The Siqueiros and mean MORB values represent the average of two T_p values computed using two different estimates for melt fraction, F (Fig. 9). Our preferred estimate for the average mantle geotherm is the arithmetic average of T_p derived at Siqueiros, and that derived using mean FeO^{liq} from PETDB MORB: error analysis yields: T_p^{MOR}=1454± 78 °C, presuming Fo_{max} at Siqueiros is valid globally. We use 1454 °C to calculate mantle excess temperatures at hot spots relative to MORs.

To estimate the standard deviation of potential temperatures beneath MORs, we consider the 1σ value for MORB FeO contents, which is ±0.57 wt.% (computed for all MORB with 7 wt.% ≤ FeO ≤ 9.6 wt.%). The 1σ FeO variation about the mean MORB FeO (Fig. 9b) translates to a 1σ variation in T in the sub-MOR mantle of ±30 °C (Fig. 9b), or ±34 °C, if an uncertainty of ±0.04 on Fo_{max} is included (a ±0.04 uncertainty in Fo_{max} translates to a ±15 °C uncertainty in T). These observations indicate that a rather narrow range of temperatures characterizes the sub-MOR mantle. Our T estimates do not account for variations in H_2O beneath various MOR segments. Recent work that accounts for H_2O variations at the Azores (Asimow et al., 2004) suggests that the sub-MOR temperature range may be further diminished. As a "null hypothesis", we chose not to filter the global MORB database for hot spot effects (other than excluding Iceland). Siqueiros may indeed be more representative of mean MORB temperatures, if, as we show for Iceland, Samoa and Hawaii, that near-ridge hot spots are indeed hot. In addition, if the observed value for $K_D(Fe–Mg)^{ol\text{-}liq}$ of 0.29 at Siqueiros is valid (Fig. 6), and applies globally, then T_p for MORB (see below) is lower by 25 °C.

4.4. Sources of error: melt fraction (F) and pressure (P)

The above-noted mantle potential temperatures depend upon estimates of F and P (see Fig. 1, caption and Appendix A). Estimates of F are very uncertain (see Appendix A), and so estimates of T_p are much less accurate than estimates of olivine-liquid equilibration reported in Fig. 9 and Table 2. To estimate F we interpolate between experiments performed on peridotite bulk compositions (see Appendix A for details); an uncertainty in F of ±5% translates to a thermal uncertainty of ±33 °C. Pressure estimates also enter into the calculation of T_p, since $F=f(P,)$ and also because of a correction for adiabatic upwelling (Fig. 1).

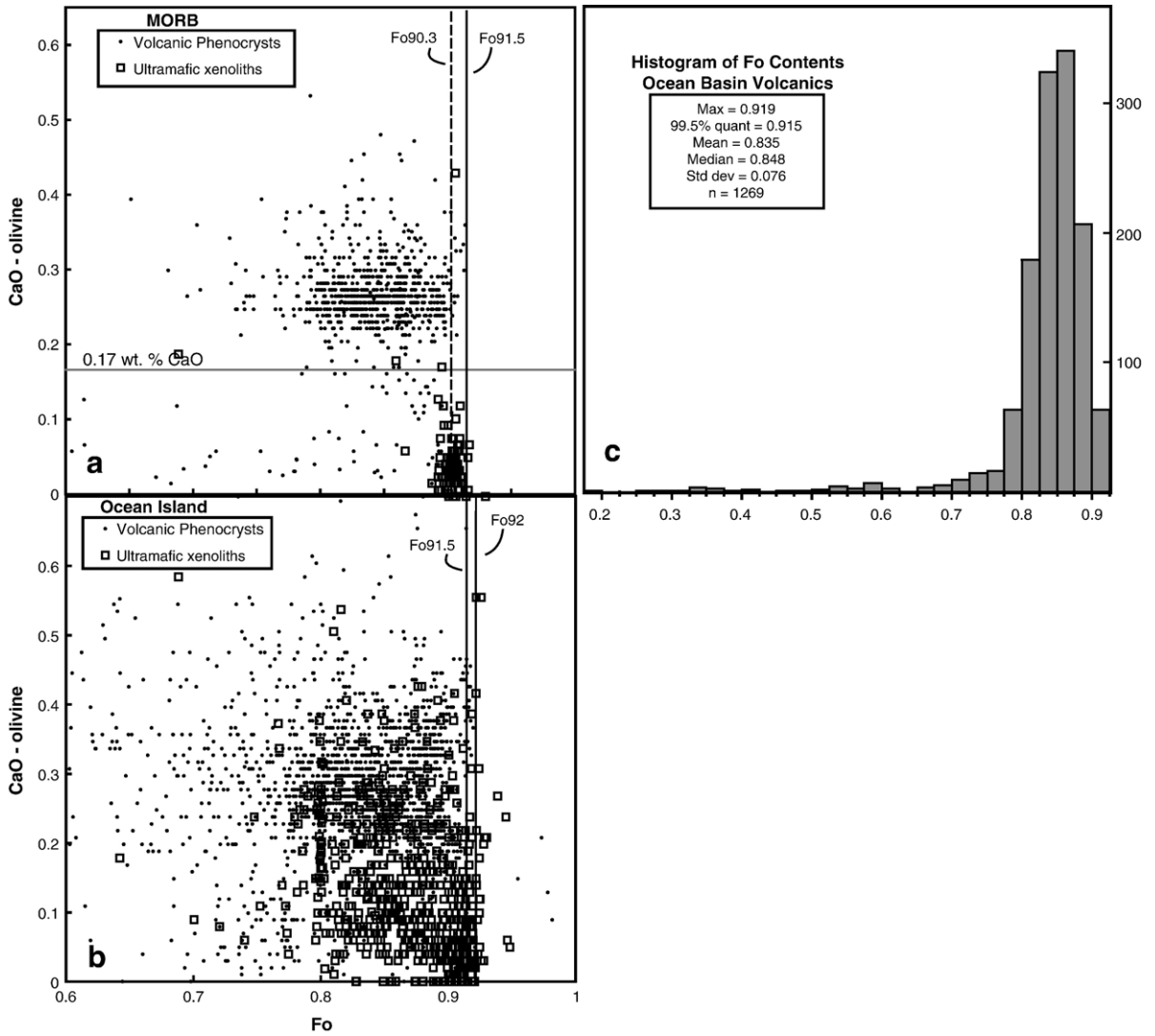

Fig. 8. Olivines from volcanic phenocrysts and ultramafic rocks (from PETDB) (a) and ocean islands (b) are compared. Ultramafic-derived olivines tend to have very low CaO, such that at MORs CaO = 0.17 wt.% can be used to separate the two populations. Note that global phenocryst Fo_{max} values overlap ultramafic olivine compositions; this indicates that global phenocryst Fo_{max} provides an appropriate estimate for the highest Fo contents achieved during mantle melting. (c) A histogram of Fo contents for phenocrysts for MORB. The non-Gaussian, steep drop off in olivines with high Fo, may reflect a natural maximum in Fo imposed by a maximum T from which MORBs are derived (Fig. 9), as well as perhaps a low variance for the mantle source composition.

However, the P assumed for olivine equilibration has little effect on estimates of T_p (Table 2). For example, though as P is increased, olivine equilibration temperatures ($T^{ol\text{-}liq}$) increase, potential corresponding increases in T_p are offset because as P increases, 1) smaller values of F are needed to generate high MgO liquids, and so the upward correction for the heat of fusion (Fig. 1) is less, and 2) there is a greater drop in T due to greater upwelling along the mantle adiabat (Fig. 1). Table 2 compares calculations of T_p for equilibration at 1 atm–5 GPa and shows that error resulting from an assumption of P (mean error is ±12 °C) is nearly negligible compared to other sources of error, such as assumed values for F, or $K_D(Fe–Mg)^{ol\text{-}liq}$.

5. Mantle excess temperatures at Hawaii, Iceland and Samoa

5.1. Methods

Putirka (2005) provided an updated version of the Roeder and Emslie (1970) thermometer to show, in

response to Green et al. (2001), that high FeO^{liq} at Hawaii and Iceland requires greater values for T_p at these localities compared to MOR's, despite similar values for Fo_{max}. The Putirka (2005) models were calibrated to test the effects of H_2O and CO_2 on calculations of T_{ex}. By applying similar fO_2 conditions and $K_D(Fe–Mg)^{ol\text{-}liq}$, Hawaii still has a considerable excess T of 168 °C. We re-calculate T_p at Hawaii and Iceland, and introduce new calculations for Samoa, using Eqs. (2) and (3), and $K_D(Fe–Mg)^{ol\text{-}liq}=0.34$ (Fig. 6b) at Hawaii and Samoa, and

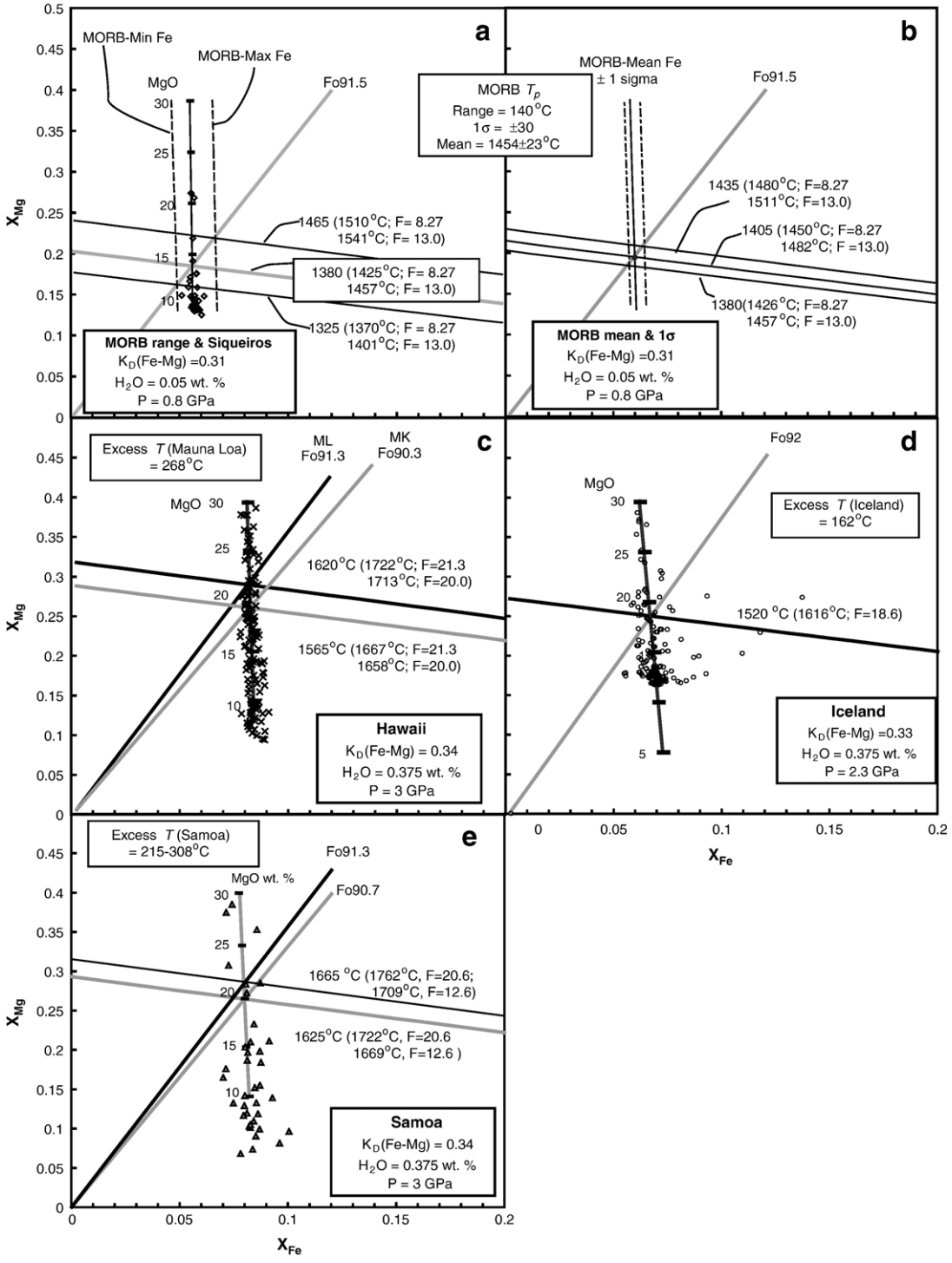

0.32 at Iceland (see Appendix A). Values for $K_D(Fe–Mg)^{ol\text{-}liq}$ at Hawaii are in part based on the observation that mean whole rock-olivine compositions are consistent with $K_D(Fe–Mg)^{ol\text{-}liq}=0.34$ (Fig. 6b); to presume a lower value for $K_D(Fe–Mg)^{ol\text{-}liq}$ introduces a mass balance problem that can be solved only if high density olivine-rich slurries are somehow preferentially erupted over their lower density, more highly fractionated counterparts (Fig. 6b). This argument is similar to that posed by Wright (1973) when he estimated that the minimum MgO content of Hawaiian parental magmas as 15.5 wt.%. A perhaps under-appreciated fact is that parental liquids must represent the sum of all erupted and non-erupted liquid and crystalline products, and if dense olivine slurries are preferentially left behind in a conduit, erupted products yield minimum estimates for parental MgO.

For consistency, we use the mean $K_D(Fe–Mg)^{ol\text{-}liq}$ derived from the models of Herzberg and O'Hara (2002), Toplis (2005), and Putirka (2005) to all localities (including MORB; see Appendix A), which at Hawaii matches the observed value. We also presume equilibration at 3 GPa, or near the base of the lithosphere for Hawaii and Samoa, and 2.3 GPa, at Iceland. As noted for MORB, though, T_p estimates are nearly independent of the assumed P of olivine-liquid equilibration (Table 2). In any case, high P, and elevated values for $K_D(Fe–Mg)^{ol\text{-}liq}$ (due to high P–T; e.g., Herzberg and O'Hara, 1998) at hot spots overlying thick lithosphere are probably the most realistic. Studies show that clinopyroxenes can be transported from well below the base of the crust (e.g., Putirka, 1997; MacLennan et al., 2001b, Klügel and Klein, 2006). High Fo olivines, which by any method yield higher temperatures than clinopyroxenes, are thus almost certainly mantle-derived, probably from greater depths than the greatest depths inferred for clinopyroxenes.

At Hawaii, we use data from the Hawaii Scientific Drilling Project (HSDP) and from Norman and Garcia (1999). At Iceland we use data from MacLennan et al. (2001a) and the GEOROC database. At Samoa we use data from the GEOROC database and new analyses of picritic samples. To calculate FeO, we apply the fO_2 conditions of Rhodes and Vollinger (2005) for Hawaii and presume that the same conditions characterize Samoa (FeO=0.92[FeOt] on a weight % basis) and at Iceland (and MORB) we apply the fO_2 conditions of Bezos and Humler (2005) (FeO=0.88[FeOt]). Finally, we calculate Fe^{3+}/Fe^{2+} ratios using the model of Kress and Carmichael (1988) (see Appendix A for details).

5.2. Temperatures at Hawaii, Iceland and Samoa

Olivine equilibration temperatures at 3 GPa at Mauna Loa, Hawaii and at Samoa are 1620 °C and 1625 °C respectively. At Iceland, olivine equilibration at 2.3 GPa is 1520 °C (Fig. 9). Our method implies a value for the MgO content of parental magmas at each locality, which can be used to estimate a parental magma composition (Table 1), as well as melt fraction and a mantle potential temperature (see Appendix A). Our calculated mantle potential temperatures are insensitive to P (Table 2), but sensitive to very uncertain estimates of F. Mantle potential temperatures at Hawaii and Samoa are estimated to both be 1722 °C, while at Iceland our estimate is 1616 °C. These estimates exceed MOR maximum T_p values by 105–211 °C and imply mantle excess temperatures, T_{ex}, of 268 °C at Hawaii and Samoa, and 162 °C at Iceland. These temperatures rise so far above average and maximum values for T_p^{MOR} that volcanism at Iceland, Samoa and Hawaii appear almost certain to derive from thermally driven mantle plumes. These conclusions account for variations in water contents between MOR and hot spot sources, and are robust against variations in CO_2 and other major mantle components, and, except for estimates of F, are independent of any assumed composition for their mantle sources (see Putirka, 2005; Appendix A).

Opponents to the plume hypothesis might still posit that fO_2 variations might account for the apparent thermal differences. But oxidation states of one log unit above the quartz–fayalite–magnetite buffer (QFM+1) would be required to explain the proposed model of Mauna Loa compositions by Green et al. (2001) in the case that $K_D(Fe–Mg)=0.30$; even higher oxidation states are required in the more likely case that $K_D(Fe–Mg)$ approaches 0.34 or 0.35.

Fig. 9. Olivine saturation models (using the approach detailed in Putirka, 2005) are used to estimate temperatures at MORs (a) and (b), Mauna Loa and Mauna Kea at Hawaii (c), Iceland (d), and Samoa (e). The axes, X_{Mg} and X_{Fe} are the cation fractions of MgO and FeO for glass or whole rock compositions. Near-vertical lines are regression lines through various data subsets; MgO contents are recovered as shown in Fig. 2, and marked along the regression lines. (a) Shows the range of MORB temperatures calculated using the global range of primitive FeO^{liq} (Fig. 7). (b) Shows MORB temperature estimates using the mean $\pm 1\sigma$ variations for primitive MORB with $FeO^{liq}=7–9.6$ wt.%. Temperatures of olivine equilibration are given next to the isotherms (nearly horizontal lines); these temperatures are converted to mantle potential temperatures, which are shown in parentheses (see Fig. 1 and Appendix A for calculation strategy) using Eq. (A1) to calculate F. For MORB we show calculations using A1 and A2 (see Appendix A for calculation details). In (c), Fo_{max} is 91.3 at Mauna Loa (Baker et al., 1996; this study) and 90.3 at Mauna Kea (this study). Water contents for the mantle source are inferred from (Dixon et al., 2002). In each graph, the thermometers require estimates for SiO_2^{liq} and $(Na_2O+K_2O)^{liq}$; these are given in Table 1and are explained in Appendix A.

Table 2
Calculated T(°C) for olivine equilibration, T_{eq}, and mantle potential temperature, T_p

	Siqueiros-A1	Siqueiros-A2	Iceland-A1	Hawaii-A1	Samoa-A1	Samoa-A2
$T_{eq}[T_p](F)$ at 5 GPa	1455[1404](1.5)	1455[1412](2.6)	1565[1599](14.3)	1665[1719](18.1)	1665[1661](9.4)	1665[1704](15.9)
$T_{eq}[T_p](F)$ at 4 GPa	1435[1407](3.1)	1435[1419](5.0)	1550[1608](15.9)	1645[1723](19.7)	1645[1665](11.0)	1645[1713](18.2)
$T_{eq}[T_p](F)$ at 3 GPa	1423[1418](4.7)	1423[1435](7.3)	1525[1605](17.5)	1620[1722](21.3)	1625[1669](12.6)	1625[1722](20.6)
$T_{eq}[T_p](F)$ at 2 GPa	1400[1418](6.3)	1400[1440](9.6)	1510[1613](19.1)	1605[1731](23.0)	1605[1673](14.2)	1605[1731](22.9)
$T_{eq}[T_p](F)$ at 1 GPa	1380[1420](7.9)	1380[1447](12.0)	1490[1616](20.7)	1585[1736](24.6)	1585[1677](15.8)	1585[1740](25.2)
$T_{eq}[T_p](F)$ at 1 atm	1365[1428](9.6)	1365[1460](14.3)	1475[1624](22.3)	1565[1740](26.2)	1570[1686](17.4)	1570[1754](27.6)
Average T_p(C)	1416	1435	1611	1728	1672	1727
S.D.	8.9	18	8.8	8.5	9.0	18
Excess T_{ex}(C)	–	–	176–195	293–312	237–256	292–311

F is in percent and calculated using Eqs. (A1) or (A2), as indicated in header (see Appendix A).
Olivine equilibration temperatures, T_{eq}(°C), are calculated using models (2) and (3), and the liquid compositions in Table 1. We use constant values for $K_D(Fe–Mg)^{ol\text{-}liq}$ (MORB = 0.31; Hawaii and Samoa = 0.34; Iceland = 0.32) and Fo_{max} (Fig. 9) and presume that fO_2 is buffered (see Appendix A). Mantle potential temperatures, T_p(°C), are calculated from T_{eq} using the equations of Fig. 1, and models for melt fraction, F, where $F = f(P,C_i)$, where P is pressure, and C_i are weight percent composition terms, from Table 1; see Eqs. (A1) and (A2) in Appendix A.

Hawaiian lavas, though, are if anything less oxidized than QFM (Rhodes and Vollinger, 2005), and K_D(Fe–Mg) is unlikely to be as low as 0.30 (Fig. 6b). It thus appears inescapable that excess temperatures at Hawaii (and Iceland) are very high, and that variations in fO_2 (Fig. 10), H_2O, CO_2 and other major mantle components (Putirka, 2005) are incapable of erasing these differences.

6. An upper mantle convective geotherm

Our estimate for T_p^{MOR} should reflect the temperature of the upper mantle in all regions thermally unperturbed by subduction or rising plumes. As a test, we compare our estimate of T_p^{MOR} to mantle temperatures derived by other means (Fig. 11). Interestingly, though our estimates of T_p beneath MORs exceed some published estimates, they are consistent with geophysical observations: Temperature estimates from heat flow and sea floor bathymetry (1450 ± 250 °C at 90 km depth; Stein and Stein, 1992), match well with our proposed MOR geotherm. Unfortunately, the temperature of the olivine–spinel phase transition is uncertain due to uncertainty related to water contents (e.g., Smyth and Frost, 2002), mantle composition (Thybo et al., 2003; Frost, 2003) and the placement of phase boundaries (Bina and Helffrich, 1994). Indeed, Cammarano et al. (2003) conclude that inversion of seismic velocities at the 410 km discontinuity for temperatures is "unreliable." Jeanloz and Thompson (1983) suggested a T of 1427 ± 300 °C, which is consistent with the later experiments of Ito and Katsura (1989), and probably still reflective of current uncertainties, and which overlaps our T_p^{AMG}. Temperature estimates appear somewhat more certain at 670 km. Da Silva et al. (2000) estimate temperatures for a pyrolite (PYR) and a silica enriched (Hi Si) mantle (Fig. 11). The downward extrapolation of our geotherm would appear to support a layered mantle that is enriched in SiO_2 below 670 km. However, Hirose's (2002) experiments on a pyrolite mantle composition show that the majorite–perovskite phase transition, having a positive Clapeyron slope, complicates the picture. Hirose's (2002) experiments are consistent with

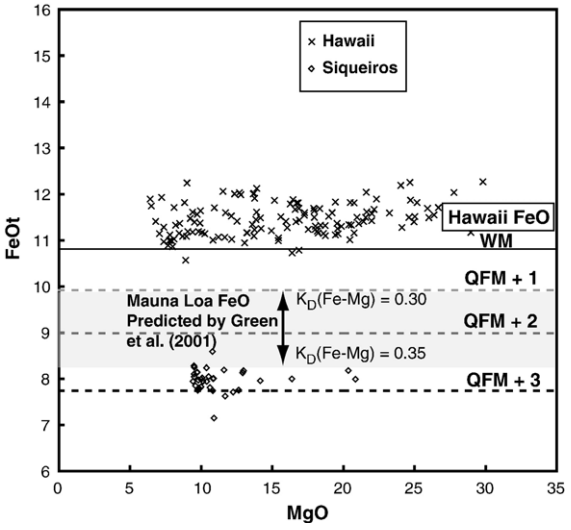

Fig. 10. FeOt (FeO total) vs. MgO for Hawaii and Siqueiros lavas (Data as in Fig. 5). Since Fo_{max} is similar at MORs, Iceland and Hawaii, variations in T are controlled largely by variations in Fe. FeO contents can thus be used to test the reasonableness of estimates of T_{ex}. Calculations show that for the Mauna Loa model of Green et al. (2001) to be valid, fO_2 at Hawaii would need to approach 1 log unit above the quartz–fayalite–magnetite (QFM + 1) buffer, for $K_D(Fe–Mg)^{ol\text{-}liq} = 0.30$; even higher oxygen fugacities are required if $K_D(Fe–Mg)^{ol\text{-}liq} = 0.34$ or 0.35. But Rhodes and Vollinger (2005) have shown that Hawaiian lavas are more reduced than QFM. It is similarly unreasonable to call upon fO_2 to yield overlapping FeO^{liq} at Samoa and Siqueiros.

a 1600–2000 °C T range at 670 km, and hence are consistent with our MOR geotherm, and a pyrolite lower mantle. Perhaps more importantly, Hirose's (2002) results suggest that the 670 km discontinuity is unlikely to be uplifted if T_{670}=1800 °C. Seismologists use the observation of a shallow "670 km" seismic discontinuity as evidence of a thermal anomaly in the lower mantle (based on the negative Clapeyron slope for the spinel–perovskite phase transition in simple mantle systems), and a flat 670 km discontinuity to suggest the absence of a thermal anomaly. However, Hirose's (2002) work shows that the Clapeyron slopes of spinel/post-spinel phase changes in a pyrolite composition mantle are such that even if the 670 km discontinuity is not anomalously shallow, excess temperatures might still be rooted in the lower mantle. Finally, Hofmeister (1999) uses thermal conductivity models to calculate a geotherm with a comparatively high implied T_p for a dry mantle (Fig. 11). The errors on this geotherm are unclear, and

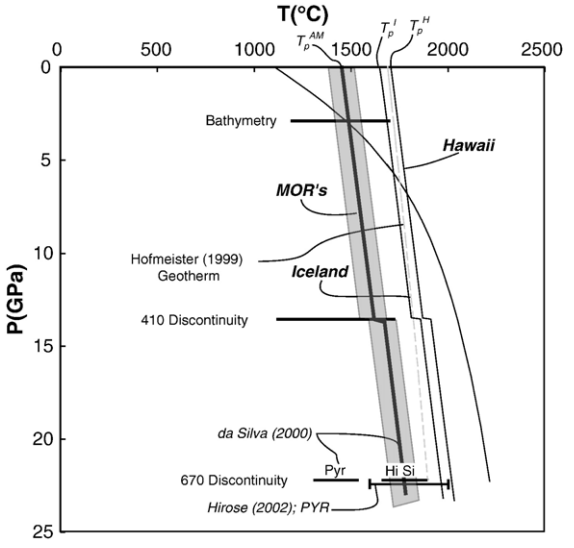

Fig. 11. The T_p estimated for MORs is likely to reflect the T of the convective mantle geotherm. Our proposed geotherm is compared to T estimates derived from the coincidence of seismic discontinuities at 410 km and 670 km with associated phase transitions, and the geotherm proposed by Hofmeister (1999). $T_p^{AMG}=T_p$ of Average Mantle Geotherm, and is derived from MORBs; $T_p^{I}=T_p$ of Iceland; $T_p^{H}=T_p$ of Hawaii. The gray field about T_p^{AMG} indicates error on the estimate of T_p^{AMG}. The inflection at 410 km reflects the anticipated 50 K increase in T (Frost, 2003) due to the exothermic phase change of olivine to wadsleyite, the spinel form of $(Mg,Fe)_2SiO_4$. This drop in T can be computed from an expression similar to that used in Fig. 1 to calculate the T drop upon melting, i.e., $\Delta T \approx F(\Delta H_r/C_p) = -T(\partial P/\partial T)(F)(\Delta V_r)/C_p$, where F=the fraction of olivine in mantle peridotite (that converts to spinel), T is the temperature of reaction, ΔH_r and ΔV_r are the enthalpy and volumes of reaction, C_p is heat capacity and $\partial P/\partial T$ is the Clapeyron slope of the olivine–spinel phase transition.

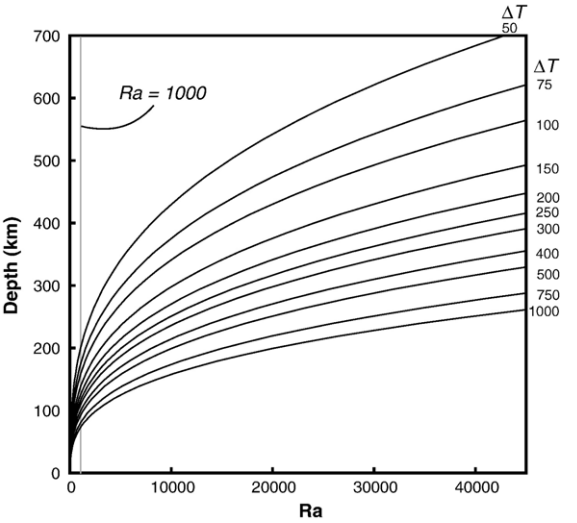

Fig. 12. Estimates of excess temperatures, T_{ex}, can be used as minimum estimates of ΔT, in calculating thermal buoyancy from the Rayleigh number, Ra. Such calculations show that Ra becomes supercritical ($Ra_c \approx 1000$) at depths that are much more shallow than likely sites of plume nucleation, i.e., the 670 km discontinuity, or the core/mantle boundary.

it is also uncertain that the small amounts of water presumed for the upper mantle (Dixon et al., 2002) would bring her geotherm and ours into agreement (Fig. 11). Our mantle potential temperatures are also lower than those implicit in Fig. 1 of Jeanloz and Morris (1986; ≈1477–1630 °C "cold", and ≈2100–2200 °C "hot"), but appear to reside within their stated errors.

Another test is to compare initial melting depths that are implied by our T_p calculations, with those derived from seismic detection of low velocity zones in the mantle. Initial melting depths are calculated from the intersection of our convective geotherms with the mantle solidus. Hirschmann (2000) has reviewed experiments that delimit the dry mantle solidus. His quadratic fits to the data have the unfortunate feature of a thermal maximum, which we rectify by fitting Hirschmann's (2000) data using the functional form of McKenzie and Bickle (1988):

$$P(\text{GPa}) = \frac{T(°\text{C}) - 1120}{157.17} + 1.596 \times 10^{-1}\left[\exp\left(4.169 \times 10^{-3}\{T(°\text{C}) - 1120\}\right)\right] \quad (6)$$

Eq. (4) reproduces Hirschmann's "Recommended Fit" for the solidus at $P<10$ GPa (his Table 1), and is consistent with Herzberg and Zhang's (1996) solidus estimates above 10 GPa. Depths are converted from P using PREM (Anderson, 1989).

Our values for T_p imply initial melting depths (at the dry solidus) of 220 km beneath Hawaii, 160 km beneath Iceland, and 95 km beneath MORs. The latter estimate matches almost precisely the seismic estimate for the base of the zone of "primary melting" (at 100 km; MELT Seismic Team, 1998) and is consistent with geochemical evidence that requires melting in the garnet stability field (e.g., Salters and Hart, 1989). The MELT Seismic Team's zone of "incipient melting" extends to 150 km, and is likely controlled by mantle volatile contents. Unfortunately, no seismic experiment comparable to that of the MELT Seismic Team (1998) study has been performed at Iceland or Hawaii. Current work suggests that our calculated initial melting depths are at least plausible (e.g., Laske et al., 1999; Foulger et al., 2000), but higher resolution studies are needed to provide a test of low velocity zone depths (Laske et al., 1999; Priestley and Tilmann, 1999; Ritsema and Allen, 2003).

In summary, our proposed geotherm is thus consistent with sea floor bathymetry, known mantle phase transitions and seismically inferred melting depths. By all appearances, our proposed geotherm carries much less uncertainty ($\approx \pm 78$ °C for estimates of mean T_p) than other methods. We thus suggest that our proposed geotherm could be used as a constraint upon models of upper mantle convection, composition, mineralogy, and thermal conductivity.

7. Active vs. passive upwelling

Given an estimate for the mantle geotherm, does there exist some minimum threshold T_{ex}, above which active upwelling is assured? Given that thermal plumes may cool en route to the surface (Leitch et al., 1996; Albers and Christensen, 1996), estimates of T_{ex} provide minimum estimates of ΔT (the temperature difference across a layer of thickness D) when calculating a Rayleigh number (Ra); Ra gives the balance between buoyancy forces that enable, and inertial forces that inhibit, convection. We let D, the depth of the convecting layer, vary for a given value of ΔT, and determine the critical depth (D_c) at which Ra becomes supercritical ($Ra_c \approx 1000$), and calculate Ra using: $Ra = \frac{g\rho D^3 \Delta T}{\kappa\mu}$, where g is acceleration due to gravity, ρ is density (3300 kg/m^3), κ is thermal diffusivity (10^{-6} m^2/s) (see Davies, 1999) and μ is viscosity (3.9×10^{20} Pa·s; King, 1995; King (1995) reports a range of viscosities of 2×10^{19}–1×10^{21}). For T_{ex} at Hawaii and Samoa (268 °C) and Iceland (162 °C), Ra reaches 1000 at depths of 114 and 135 km respectively (Fig. 12). If circulation encompasses the entire upper mantle (D=670 km; then Ra=14.1×10^3 at Iceland and 18.6×10^3 at Hawaii) or the entire mantle, Ra_c values are well above critical. These calculations suggest that Hawaii, Samoa and Iceland result from active upwellings. Our T estimates do not delimit the depths at which thermal anomalies are nucleated. But to use Iceland as an example, even plume skeptics agree that low seismic velocities extend to at least the base of the upper mantle (Foulger et al., 2000). If low seismic velocities reflect temperature variations, then it seems safe to conclude that thermally driven active upwellings extend to at least to the base of the upper mantle.

8. Comparisons to some prior petrologic T_p estimates

Our present work finds agreement, but also important differences, with several recent and early studies. Our parental liquid compositions for MORB and Hawaii are remarkably similar to the "primary magma" compositions proposed by Herzberg and O'Hara (2002) (our definitions for "primary" and "primitive" magmas overlap; see Appendix A). Our parental magma compositions at Hawaii are also consistent with the minimum MgO (15 wt.%) estimates established by Wright (1973) and Clague et al. (1991). Our estimates for T_{ex} are also very similar to those estimated by Herzberg and O'Hara (1998) and MacLennan et al. (2001a). In addition, we find agreement with the 250 °C T range estimated by Klein and Langmuir (1987) for T^{Iceland}–$T^{\text{coldest MORB}}$: our estimate for T^{Iceland}–$T^{\text{coldest MORB}}$ is 215–246 °C (Fig. 9). In contrast, the global MORB T ranges of 100–140 °C inferred by Presnall et al. (2002) and Shen and Forsyth (1995) include Iceland, and hence are far too small to explain the global range of MORB olivine equilibration temperatures calculated here (Fig. 9). Shen and Forsyth (1995) appear to overestimate the influence of mantle heterogeneity. Presnall et al. (2002) appear not to account for the heat of fusion in calculating T_p, and it would also appear that phase compositions and proportions inferred from synthetic systems do not extrapolate precisely to natural systems.

As for absolute T estimates, we find agreement with Wang et al.'s (2002) estimate of $T^{\text{ol-liq}}$(2.2 GPa)=1435 °C at the East Pacific Rise (their T_p=1448 °C, if F=6%; compared to our value of T_p=1454 °C), and Leeman et al.'s (2005) study of the Cascades implies that T_p=1400 °C, or higher, depending upon F. But Herzberg and O'Hara (2002) estimate lower temperatures for MORB (T_p=1380 °C) and lower values for T_{ex} at Kilauea, Hawaii (140–190 °C). Our differences with Herzberg and O'Hara (2002) are largely due to the conversion of an olivine-liquid temperature, $T^{\text{ol-liq}}$, to a mantle potential temperature, T_p. (As shown in the Appendix A, various thermometers yield

similar $T^{ol\text{-}liq}$ estimates when consistent input data are used, especially at elevated P). For example, using Herzberg and O'Hara's (2002) Kilauea sample 2E, (their Table 5), which is similar to our preferred parental liquid, they estimate that $F=14\%$ at 3.3 GPa and that $T^{ol\text{-}liq}$ (4 GPa)=1651 °C. Using their F and the parameters of Fig. 1, we calculate that $T_p=1700$ °C, which would be in agreement with our preferred estimate of $T_p^{Hawaii}=1722$ °C. Though unclear, it appears that Herzberg and O'Hara apply $F=14\%$ at 1 atm to correct their 1 atm estimate for $T^{ol\text{-}liq}=1467$ °C, which from Fig. 1 yields $T_p=1560$ °C. Our interpolation of experimental data (Eq. (A1)) indicates, however, that F at 1 atm is 26.5%, which when applied to their $T^{ol\text{-}liq}$ (1 atm), yields $T_p=1644$ °C, much closer to our preferred value; the remaining difference at 1 atm is because Eq. (2) predicts a higher T than Beattie (1993) (see Appendix A). More interestingly, had Herzberg and O'Hara (2002) simply made their corrections from $T^{ol\text{-}liq}$ to T_p at elevated P, they would derive a T_p nearly identical to ours: From their Table 5: $F_{mean}=21.7\%$, and $T^{ol\text{-}liq}_{mean}$ (4 GPa)=1634 °C, which (using Fig. 1) converts to $T_p^{Kilauea}=1725$ °C, nearly identical to our $T_p^{Hawaii}=1722$ °C. We suggest that 1) Herzberg and O'Hara's (2002) estimates for T_p at Kilauea (1520–1570 °C) are too low due to an underestimate of F, especially at 1 atm, and 2) that the discrepancy is rectified by considering their mean values for F and $T^{ol\text{-}liq}$ at elevated P. More significant is our departure with Green et al. (2001), who estimate that $T_{ex}\approx 0$ °C (see also comparisons to Falloon et al. (this volume) in Appendix B). However, Green et al.'s (2001) implicit estimates for FeOt at Hawaii are very low, requiring unacceptably high values for fO_2 (Fig. 10). Green et al. (2001) also do not appear to correct for the heat of fusion when calculating T_p, and implicitly select a low value for Fo_{max} at Hawaii, by averaging temperature estimates for volcanoes that are not directly over the hot spot.

9. Summary

The key issue in the plume debate is whether mid-plate volcanic activity is caused by passive, or thermally driven active upwellings. These models are distinct in that thermally driven upwellings will exhibit excess temperatures that reflect excess heat in their mantle source regions. We propose an observation-driven approach, and updated olivine-liquid thermometers to estimate mantle temperatures and identify mantle plumes. Key observations include estimates of parental FeO^{liq}, as inferred from olivine control lines (Figs. 5 and 7), maximum Fo contents recovered from primitive magmas or mantle xenoliths (Fig. 8), and values for $K_D(Fe\text{–}Mg)^{ol\text{-}liq}$ determined from mass balance considerations (Fig. 6). Our T estimates are not entirely model-independent, as they require (in addition to a geothermometer) an estimate of fO_2 and, for precision, an estimate of a parental liquid composition. Our potential temperature, T_p, for the average mantle geotherm, which we derive from Siqueiros, and mean FeO contents from MORBs ($Fo_{max}=91.5$) is $T_p^{AMG}=1454\pm 78$ °C. This value defines the convective geotherm that should apply at any locality that has not been thermally disturbed by subduction or active mantle upwelling. Global variations in sub-MOR temperatures have a range of 140 °C, but a very narrow 1σ variation of ±34 °C. Clearly, there is support for the view that isotherms are nearly flat at depth in thermally undisturbed regions of the upper mantle (McKenzie, 1967; Ahern and Turcotte, 1979; McKenzie and Bickle, 1988). Our calculations for $T^{Iceland}$–$T^{coldest\ MORB}$ (215–246 °C) further support the Klein and Langmuir (1987) view that temperature variations ($T^{Iceland}$–$T^{coldest\ MORB}=250$ °C) control global variations in FeO, Na_2O and SiO_2, and that parental MORB liquids are picritic, and produced at high temperatures (O'Hara, 1968; Jacques and Green, 1980; Stolper, 1980).

Potential temperatures at Hawaii and Samoa are 1722 °C and at Iceland is 1616 °C, and exceed even the highest temperatures estimated for MORBs by >100 °C. A source of excess thermal energy seems inescapable. These excess temperatures are favored by us because they explain the coincidence at some hot spots of high excess topography (Sleep, 1990; Schilling, 1991; Watson and McKenzie, 1991), and primitive liquids that contain (a) high TiO_2/Na_2O and high Sm/Yb ratios (Putirka, 1999), and (b) high FeO, and low SiO_2 contents (Langmuir et al., 1992; Albarede, 1992). What is particularly compelling is that Ti/Na ratios are controlled by clinopyroxene-, and Sm/Yb ratios by garnet-liquid equilibria. If excess temperatures were non-existent, it would be a cruel happenstance that petrologic indicators of high P–T partial melting would be apparent, but lack such a meaning.

Our T estimates do not indicate whether or not plumes nucleate at the core–mantle boundary. However, Morgan (1971) might be correct about the basic mechanism, and also wrong about the site of plume nucleation: The concept of a layered mantle, with plumes nucleating at 670 km, is not new (Allegre and Turcotte, 1985), and has not been entirely discarded (e.g., Tackley, 2000). Since it is unclear that Earth's core contributes mass to mantle upwellings, we suggest that perhaps the only signal from the core may be thermal in nature, and that dynamic modelers investigate whether there is a critical value for T_{ex} beyond which plume nucleation at the core–mantle boundary is assured.

Acknowledgements

KDP acknowledges support from NSF grant EAR 03347345, and grants from the College of Science and Mathematics, California State University Fresno. MRP's research has been supported by OCE grants 9019154 and 0138088. FJR's participation was performed under the auspices of the U.S. Department of Energy by University of California Lawrence Livermore National Laboratory under contract No. W-7405-Eng-48, and supported by the LLNL Laboratory Directed Research and Development Program. We thank Paul Asimow, Leonid Danyushevsky, Trevor Falloon, Claude Herzberg, and Ian Ridley for very helpful discussions. Unpublished data generously supplied by Falloon et al., were useful in the early phase of the development and testing of the models presented in this work. The paper also greatly benefited from formal reviews by Trevor Falloon, J. Michael Rhodes, and an anonymous reviewer.

Appendix A. Methods

A.1. Calculation of FeOt (FeO total) and Fe^{3+}/Fe^{2+}

Iron in volcanic rocks is variously reported as Fe_2O_3t, FeOt (t for "total") or some combination of Fe_2O_3 and FeO. For consistency, we recast all Fe analyses as FeO total: we convert all oxides to a cation fraction, where, for example, reported Fe_2O_3 and FeO contents are divided by the molecular weights of $FeO_{1.5}$ and FeO respectively (and Al_2O_3, Na_2O and K_2O are respectively divided by the molecular weights of $AlO_{1.5}$, $NaO_{0.5}$, and $KO_{0.5}$, etc.). We calculate the cation sum, $FeOt^{cs} = FeO_{1.5} + FeO$, and multiply $FeOt^{cs}$ by the molecular weight of FeO, and similarly weight all other oxides by their respective molecular weights. Renormalization to 100 yields weight percent values for FeOt, which is used for all subsequent calculations, and all graphs in this paper. When Fe_2O_3 and FeO are both reported, and $Fe_2O_3/(Fe_2O_3+FeO) < 10\%$ by weight, then if FeOt is calculated as Fe_2O_3+FeO, the error is less than 1%.

To calculate Fe^{2+}/Fe^{3+} and $Fe^{2+}/(Fe^{2+}+Fe^{3+})$ from FeOt, we use the expressions of Kress and Carmichael (1988). Since Fe^{2+}/Fe^{3+} varies with T, we apply an iterative procedure: we calculate $Fe^{2+}/(Fe^{2+}+Fe^{3+})$ over a range of temperatures using our model compositions (Table 1) and natural compositions reported in Rhodes and Vollinger (2005) and Bezos and Humler (2005). We apply the fO_2 conditions inferred by the aforementioned studies and presume that fO_2 is buffered. We then use a calculated value for T to infer the cation ratio Fe^{2+}/Fe^{3+}, and then use this new value of Fe^{2+}/Fe^{3+} to recalculate T. Because of the greater molecular weight of Fe_2O_3 compared to FeO, a 2% change in the weight ratio translates to approximately a 1% change in the cation ratio $Fe^{2+}/(Fe^{2+}+Fe^{3+})$.

A.2. Calculation of parental magma compositions

The method of T estimation of Putirka (2005) implies a (predicted) value for MgO^{liq} for parental magmas, which can be used to calculate other oxides. We use the term "parental" in that our liquid compositions in Table 1 represent the liquids that are parental to all observed and buried volcanic and crystalline products related to mantle melting. Our liquids in Table 1 would also represent the mean compositions of what are sometimes called "primary" liquids, which are generated in the mantle, pooled, and then delivered towards the surface. An alternative term might be "pooled primary liquids."

To reconstruct a parental magma, we first determine the MgO content of the parental magma. Since FeOt is invariant along olivine control (Fig. 5), FeOt along an olivine control line (a variation trend controlled by olivine addition/removal only; Figs. 5 and 7) is equivalent to $FeOt^{parental\ liquid}$ or $FeOt^{pl}$. With a calculated value for $K_D(Fe–Mg)^{ol\text{-}liq}$, we use $FeOt^{pl}$ and observed Fo_{max} to yield a unique value for MgO^{pl} (independent of any model for T or mantle composition): Fo_{max} fixes the value for Fe/Mg of olivine, and with $(Fe/Mg)^{ol}$ the value for $K_D(Fe–Mg)^{ol\text{-}liq}$ fixes the value of Fe/Mg for the liquid. If $FeOt^{pl}$ (and fO_2) are known, then MgO^{pl} is fixed by these values. Similarly, given estimates for MgO^{pl}, Fo_{max} and $K_D(Fe–Mg)^{ol\text{-}liq}$, one may calculate $FeOt^{pl}$, which is how we test the model of Green et al. (2001) (Fig. 10). To reconstruct the remaining parental magma components, we add olivine to a "primitive" lava until the predicted MgO content is achieved. Primitive lavas are derived from a mean of natural lava compositions that are sufficiently MgO rich to be on an "olivine control" line. We use the following MgO values as delimiters for our primitive liquids; Siqueiros: 9–10.5 wt.%; Iceland: 9.5–11.5 wt.%; Hawaii: 8–10 wt.%; Samoa, 8.75–1.5 wt.%. Since olivine control lines represent mixtures, not liquid lines of descent, we do not perform a "reverse fractionation model", which would have no meaning. We use Fig. 5 to determine the mean Fo content along an olivine control line, and use this Fo for correction. This choice enforces that our liquids in Table 1 will always lie within observed major oxide variation diagrams. We emphasize that whole rocks that have MgO^{pl} values are unlikely to be liquids: They are mixtures that have the appropriate MgO^{pl} only by accident, not by virtue of evolution.

A.2.1. Estimating K_D(Fe–Mg)$^{ol\text{-}liq}$

Tests show that none of the recent models developed to predict K_D(Fe–Mg)$^{ol\text{-}liq}$, i.e., Herzberg and O'Hara, 2002; Putirka, 2005; Toplis, 2005, capture internal variations in K_D(Fe–Mg)$^{ol\text{-}liq}$. Regression analysis of experimental data (n=1007, Fig. 3) for K_D(Fe–Mg)$^{ol\text{-}liq}$(measured) vs. K_D(Fe–Mg)$^{ol\text{-}liq}$(calculated) shows that all three models yield R^2<0.04, slopes of regression lines that are embarrassingly flat (<0.4), and standard errors of estimate that are ±0.06. None of these models can be intrinsically preferred over the other, and are poor substitutes for observations (Fig. 6). Because adequate data are not available at all localities, we make use of calculated values for consistency. We first use observed values for K_D(Fe–Mg)$^{ol\text{-}liq}$ (Fig. 6) to estimate MgO^{pl}, and then iteratively apply the mean K_D(Fe–Mg)$^{ol\text{-}liq}$ calculated from Herzberg and O'Hara (2002), Putirka (2005), and Toplis (2005). This method yields a higher than observed K_D(Fe–Mg)$^{ol\text{-}liq}$ at Siqueiros (Fig. 6); if the values for K_D(Fe–Mg)$^{ol\text{-}liq}$ in Fig. 6 are accurate, however, T_p for MORB is lower by 25 °C, and excess temperatures are greater by the same amount.

A.3. Comparison of olivine-liquid thermometers

Table A1 shows that at moderate P, when consistent input is used, various models yield estimates that are within 1σ model error. But when such models disagree, which is to be preferred? Beattie (1993) used the olivine binary to show that his two-lattice solution model is superior to the regular solution model employed by Ghiorso et al. (1983). We extend this test by comparing T estimates for melting of pure forsterite (Presnall and Walter, 1993). The modified Beattie (1993) model and Eq. (4) provides superior estimates of Fo melting. However, this comparison has limitations: natural liquids do not approach the Fo binary, so success in Fig. A1 can hardly lead to confidence in predicting T for natural samples. For example, the Beattie (1993) model yields higher temperatures than Ford et al. (1983) for Eqs. (2) and (3) for Kilauea-H at 3 GPa (Table A2) even though the Beattie (1993) model yields lower temperatures for pure Fo. And though Eq. (4) and Beattie (1993) both closely reproduce the Fo melting curve, these models disagree by as much as 115 °C (Kilauea-H at 3 GPa, Table A2). An alternative test is to consider that by applying Eq. (1) with expressions of $D_{Mg}^{ol/liq}=f(T)$ and $D_{Fe}^{ol/liq}=f(T)$, it is possible to predict not only T, but also 1) K_D(Fe–Mg)$^{ol\text{-}liq}$, since K_D(Fe–Mg)$^{ol\text{-}liq}=D_{Fe}^{ol\text{-}liq}/D_{Mg}^{ol/iq}$, and 2) the Fo content of the equilibrium olivine, since $X_{Mg}^{ol}=D_{Mg}^{ol/liq}$, $X_{Fe}^{ol}=D_{Fe}^{ol/liq}$ and $Fo=X_{Mg}^{ol}/(X_{Mg}^{ol}+X_{Fe}^{ol})$. Table A2 compares estimates of T, K_D(Fe–Mg)$^{ol\text{-}liq}$ and Fo. Note that for Kilauea-H at 3 GPa, Eqs. (4) and (5) yield suspiciously high estimates for K_D(Fe–Mg)$^{ol\text{-}liq}$ and a low value for Fo, compared to other models. The models are too inaccurate to make judgments regarding small variations in such quantities, but these comparisons may be useful at differentiating T estimates that vary by more than 1−2σ. With differences in T of 1σ or less, or small differences in predicted Fo or K_D(Fe–Mg)$^{ol\text{-}liq}$ it is probably best to average the T estimates since such differences reflect experimental and calibration error.

A.4. Conversion of olivine equilibration temperatures to mantle potential temperatures, and calculating F

Experiments show that F varies strongly with MgO content and P; to estimate F we performed regression analysis of peridotite partial melting experiments from Takahashi et al. (1993), Baker and Stolper (1994), Baker et al. (1995), Robinson et al. (1998) and Walter (1998), whose data are internally consistent, and yield the following expression:

$$F(\%) = -117.2 - 1.62P(\text{GPa}) + 2.12[SiO_2^{liq}] + 4.2[MgO^{liq}] - 3.93[FeO^{liq}]. \quad \text{(A1)}$$

In Eq. (A1), compositional parameters are in weight %; n=54, R^2=0.96 and the standard error of estimate (SEE) for F is ±4.8%. Eq. (A1) predicts values of F that approach geochemical estimates of F at Hawaii (Feigenson et al., 2003) and Iceland (MacLennan et al., 2001a). But this

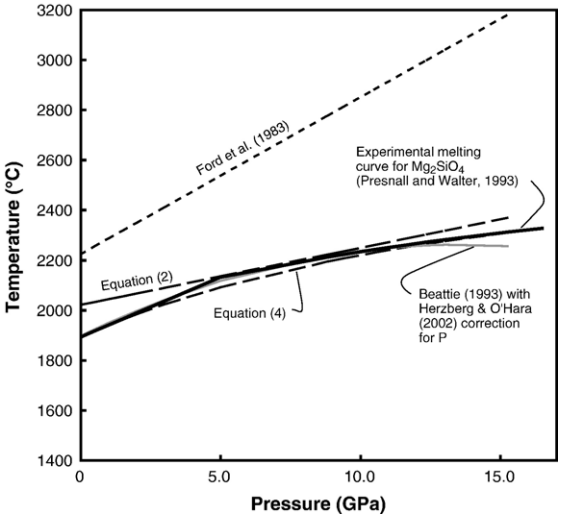

Fig. A1. Olivine-liquid thermometers (Beattie, 1993, with corrections by Herzberg and O'Hara, 2002; Eqs. (2) and (4) of this study; Ford et al., 1983) are compared for their ability to predict melting temperatures for pure forsterite (Bowen and Anderson, 1914; Presnall and Walter, 1993). The Beattie (1993) model and Eq. (4) yield the best results, but as shown in Table A2, such comparisons do not translate to systematic error on T estimates or natural samples (see Table A2).

expression predicts low values of F for MORB (7.9% at 1 GPa) compared to interpolation of just the Baker et al. (1995) data (which indicate that F is closer to 13% at 1 GPa). When data from Pickering-Witter and Johnston (2000) are included in the regression, F is less precisely recovered, but yields higher estimates of F for MORB (apparently by weighting 1 GPa data):

$$F(\%) = -105.1 - 2.34P(\text{GPa}) + 1.789[\text{SiO}_2^{\text{liq}}] + 3.84[\text{MgO}^{\text{liq}}] - 2.26[\text{FeO}^{\text{liq}}]. \quad \text{(A2)}$$

For Eq. (A2), $n=80$, $R^2=0.85$ and the SEE is ±8.3%. This expression also yields much higher estimates of F at Hawaii (>30%), and Samoa (F>20%). Since the Pickering-Witter and Johnston (2000) data may be more applicable to the high alkali lavas from Samoa, we present T_p estimates using Eq. (A2) for both MORB and Samoa (Table 2). Clearly, additional data are needed to better predict F and more precisely delimit T_p.

The calculation of F is the only part of our approach that depends upon an assumption of mantle composition, which we presume to be peridotite. Sobolev et al. (2005) have suggested that the mantle beneath Hawaii has a large fraction of a nearly olivine-free, eclogite-rich component. But eclogite or garnet–pyroxenite dominated sources are neither compatible with trace and major element, and isotopic systematics (Norman and Garcia, 1999; Norman et al., 2002; Putirka, 1999; Stracke et al., 2003), nor the large amounts of picrite lavas that occur from Mauna Kea to Koolau (Norman and Garcia, 1999; Rhodes and Vollinger, 2004; Garcia, 2002), let alone very high olivine-liquid equilibration temperatures (Putirka, 2005; this study). Until the olivine-free mantle model can meet these challenges, it is not a useful proposition.

Appendix B. Differences between this study, and Falloon et al., this volume

As with Green et al. (2001), Falloon et al. (this volume) also infer that at Hawaii, $T_e \approx 0$ °C. There are several reasons why we obtain higher T estimates for Hawaii, and T_{ex}, and why we believe their lower T estimates are incorrect: (a) Falloon et al. do not correct for the heat of fusion (Cawthorn, 1975), which is crucial to any analysis of T_p and T_{ex} (high MgO magmas are generated with greater thermal energy). (b) MgO is underestimated for Falloon et al.'s parental magma compositions at Hawaii (their Table 1): If we apply the fO_2 conditions of Rhodes and Vollinger (2005; i.e., FeO=0.92[FeOt]) and accept Falloon et al's estimate of FeOt, then even if $K_D(\text{Fe–Mg})_{\text{ol-liq}}=0.30$, a liquid with FeOt=11.8 wt.% would have 19.2 wt.% MgO for equilibrium with Fo=91.3, and 17.8% MgO, for Fo=90.7 (these calculations are model-independent). Yet Falloon et al. report that parental liquids at Hawaii have MgO=14.8 wt.%. (c) Falloon et al. use a value of Fo_{max} of 90.7 at Hawaii even though several studies have established that Fo_{max} at Hawaii is at least 91.3 (Baker et al., 1996; Garcia et al., 1995; Norman and Garcia, 1999; this work, Fig. 8). (d) Falloon et al. estimate a remarkably high value for FeOt for MORB (Fig. 5), which is well above the MORB mean, and approaches the upper 95th percentile for global MORB. Finally, Falloon et al. suggest that $K_D(\text{Fe–Mg})^{\text{ol-liq}}$ should be 0.29 at Hawaii, and 0.32 at MORs. Though Falloon et al., appear not to use these values for the calculation of T_{ex}, their suggested values contradict natural observations (Fig. 6), and the experimental data compiled for this study show that the effect of TiO_2 on $K_D(\text{Fe–Mg})^{\text{ol-liq}}$ is negligible (slope=−0.006; $R^2=0.019$) compared to T or P. Moreover, at Hawaii the lithosphere is thick (e.g., Bock, 1991, Li et al., 2004) and hence Fo_{max}-liquid equilibrium probably occurs at much greater depths compared to MORs. Regardless of whether one considers variations in $K_D(\text{Fe–Mg})^{\text{ol-liq}}$ to be driven by temperature (Sobolev and Danyushevsky (1994), pressure (e.g., Herzberg and O'Hara, 1998, Putirka, 2005), or both (Toplis, 2005), $K_D(\text{Fe–Mg})^{\text{ol-liq}}$ should be greater at Hawaii. These differences, especially (a)–(d) in the case of Falloon et al. (this volume), lead to underestimates of $T^{\text{ol-liq}}$ and T_{ex} at Hawaii.

Table A1
Comparisons of estimates for olivine equilibration temperatures and mantle potential temperatures: $T(C)^{\text{ol-liq}}$ [$T^p(C)$]; $T(C)^{\text{ol-liq}}$ are calculated from expressions of $D^{Mg}=f(T,P,X^i)$ and a liquid and olivine composition pair

	Kilauea-H	MORB-H	HSDP	Siqueiros
Fo_{max}	Fo91.3	Fo91.5	Fo91.3	Fo91.5
P (GPa)	3	0.8	3	0.8
Eq. (2) This study	1578[a][1626][b]	1356[1419]	1624[1726]	1379[1452]
Eq. (4) This study	1564[1612]	1329[1392]	1601[1701]	1345[1418]
Beattie (1993) with H&O[c]	1566[1614]	1335[1398]	1604[1706]	1352[1425]
Ford et al. (1983)	1603[1651]	1336[1399]	1655[1757]	1358[1431]
$K_D(\text{Fe–Mg})^{\text{ol-liq}}$ [d]	0.29	0.28	0.32	0.30

Table A1 (*continued*)

	Kilauea-H	MORB-H	HSDP	Siqueiros
K_D(Fe–Mg)$^{ol\text{-}liq}$ Toplis (2005)	0.32	0.28	0.32	0.28
K_D(Fe–Mg)$^{ol\text{-}liq}$ H&O[e]	0.34	0.32	0.35	0.33
K_D(Fe–Mg)$^{ol\text{-}liq}$ P(2005)[f]	0.34	0.32	0.34	0.32
Mean T_p (°C)	1626	1402	1722	1432
T_p S.D.	18	12	25	15
Excess T(°C)	224		290	

[a]$T(C)^{olivine\text{-}liquid}$ equilibrium values are calculated from expressions for $D_{Mg}=f(T,P,X_i)$, assuming liquids have equilibrated with Fo_{max} at the stated pressure. [b]T_p (brackets) is calculated from $T(C)^{ol\text{-}liq}$ and Eqs. (A1) at Hawaii and (A2) for MORB. Compositions Kilauea-H and MORB-H are primary magma compositions considered representative by C. Herzberg (pers comm.; see Table 1). HSDP and Siqueiros are from this study (Table 1). [d]$K_D(Fe–Mg)^{ol\text{-}liq}$ implied by Fo_{max} and liquid composition. [e]H&O refers to the T correction of Herzberg and O'Hara (2002) applied to the Beattie (1993) model (Beattie's Eq. (10)); [f]Putirka (2005).

Table A2
Comparison of predicted values for olivine equilibration temperatures, $K_D(Fe–Mg)^{ol\text{-}liq}$, and Fo contents: $T(C)^{olivine\text{-}liquid}[K_D(Fe–Mg)^{ol\text{-}liq}](Fo)$

	Kilauea-H	MORB-H	HSDP	Siqueiros	Excess $T(C)$[a] $K-M$	$H-S$
P (GPa)	1 atm	1 atm	1 atm	1 atm		
F	22.90% (A1)	12.80% (A1)	26.20% (A2)	14.30% (A1)		
Eqs. (2) and (3)	1528[0.34](90.2)	1347[0.32](90.6)	1568[0.35](90.9)	1368[0.32](90.9)		
T_p	1681	1432	1743	1463	249	280
Eqs. (4) and (5)	1412[0.29](91.5)	1285[0.30](91.2)	1446[0.29](92.3)	1300[0.30](91.6)		
T_p	1565	1370	1621	1395	195	226
Beattie (1993) with H&O	1505[0.31](90.9)	1367[0.31](90.7)	1535[0.31](91.7)	1381[0.31](91.1)		
T_p	1658	1452	1710	1476	206	234
Ford et al. (1983)	1456[0.31](91.0)	1330[0.31](90.7)	1486[0.31](91.8)	1346[0.31](91.1)		
T_p	1609	1415	1661	1441	194	220
Mean T_p (°C)	1628	1417	1684	1443	211	240
S.D.	52	35	53	36	26	27

	Kilauea-H	MORB-H	HSDP	Siqueiros	Excess $T(C)$ $K-M$	$K-M$
P(GPa)	3	0.8	3	0.8		
F	13.20%	10.90%	21.30%	12.40%		
Eqs. (2) and (3)	1585[0.35](90.1)	1360[0.32](90.6)	1627[0.35](90.8)	1381[0.32](90.9)		
T_p	1633	1423	1729	1454	210	275
Eqs. (4) and (5)	1570[0.36](89.8)	1332[0.33](90.3)	1602[0.35](90.9)	1347[0.33](90.8)		
T_p	1618	1395	1704	1420	223	284
Beattie (1993) with H&O	1685[0.31](90.9)	1412[0.31](90.7)	1715[0.31](91.7)	1426[0.31](91.1)		
T_p	1733	1509	1817	1499	224	318
Ford et al. (1983)	1620[0.40](88.7)	1370[0.34](90.0)	1652[0.40](89.7)	1387[0.33](90.5)		
T_p	1668	1433	1754	1460	235	294
Mean T_p (°C)	1663	1440	1751	1458	223	293
S.D.	51	49	48	32	10	18

$T(C)^{olivine\text{-}liquid}$ values are calculated from simultaneous solution of Eq. (1) and expressions of $D_{Mg}=f(T,P,X_i)$ and $D_{Fe}=f(T,P,X_i)$. Fo contents of olivine and $K_D(Fe–Mg)^{ol\text{-}liq}$ ($=D_{Fe}/D_{Mg}$) are model output. P and liquid composition are used as input. Mantle potential temperatures are calculated from $T(C)^{olivine\text{-}liquid}$ and F (from Eqs. (A1) for Hawaii and (A2) for MORB).

[a]Excess temperatures are $K-M=T^{Kilauea\text{-}H}-T^{MORB\text{-}H}$ and $H-S=T^{HSDP}-T^{Siqueiros}$.

References

Ahern, J.L., Turcotte, D.L., 1979. Magma migration beneath an ocean ridge. Earth and Planetary Science Letters 45, 115–122.

Albarede, F., 1992. How deep do common basaltic magmas form and differentiate? Journal of Geophysical Research 97, 10997–11009.

Albers, M., Christensen, U.R., 1996. The excess temperature of plumes rising from the core–mantle boundary. Geophysical Research Letters 23, 3567–3570.

Allegre, C.J., Turcotte, D.L., 1985. Geodynamic mixing in the mesosphere boundary layer and the origin of oceanic islands. Geophysical Research Letters 4, 207–210.

Anderson, D.L., 1989. Theory of the Earth. Blackwell Scientific Publications, Boston. 366 pp.
Anderson, D.L., 1998. The scales of mantle convection. Tectonophysics 284, 1–17.
Anderson, D.L., 2000. The thermal state of the upper mantle; no role for mantle plumes. Geophysical Research Letters 27, 3623–3626.
Ariskin, A.A., Frenkel, M.Ya., Barmina, G.S., Nielsen, R.L., 1993. COMAGMAT: a FORTRAN program to model magma differentiation processes. Computers and Geosciences 19, 1117–1155.
Asimow, P.D., Langmuir, C.H., 2003. The importance of water to oceanic mantle melting regimes. Nature 421, 815–820.
Asimow, P.D., Hirschmann, M.M., Stolper, E.M., 2001. Calculation of peridotite partial melting from thermodynamic models of minerals and melts, IV. Adiabatic decompression and the composition and mean properties of mid-ocean ridge basalts. Journal of Petrology 42, 963–998.
Asimow, P.D., Dixon, J.E., Langmuir, C.H., 2004. A hydrous melting and fractionation model for mid-ocean ridge basalts: application to the mid-Atlantic ridge near the Azores. Geochemistry, Geophysics, Geosystems 28. doi:10.1029/2003GC000568.
Baker, D.R., Eggler, D.H., 1987. Compositions of anhydrous and hydrous melts coexisting with plagioclase, augite, and olivine or low-Ca pyroxene from 1 atm to 8 kbar; application to the Aleutian volcanic center of Atka. American Mineralogist 72, 12–28.
Baker, M.B., Stolper, E.M., 1994. Determining the composition of high-pressure mantle melts using diamond aggregates. Geochimica et Cosmochimica Acta 58, 2811–2827.
Baker, M.B., Grove, T.L., Price, R., 1994. Primitive basalts and andesites from the Mt. Shasta region, N. California: products of varying melt fraction and water content. Contributions to Mineralogy and Petrology 118, 111–129.
Baker, M.B., Hirschmann, M.M., Ghiorso, M.S., Stolper, E.M., 1995. Compositions of near-solidus peridotite melts from experiments and thermodynamic calculations. Nature 375, 308–311.
Baker, M.B., Alves, S., Stolper, E.M., 1996. Petrography and petrology of the Hawaii Scientific Drilling Project lavas: inferences from olivine phenocryst abundances and compositions. Journal of Geophysical Research 101, 11715–11727.
Bartels, K.S., Kinzler, R.J., Grove, T.L., 1991. High pressure phase relations of primitive high-alumina basalts from Medicine Lake volcano, northern California. Contributions to Mineralogy and Petrology 108, 253–270.
Beattie, P., 1993. Olivine-melt and orthopyroxene-melt equilibria. Contributions to Mineralogy and Petrology 115, 103–111.
Bezos, A., Humler, E., 2005. The Fe^{3+}/Fe ratios of MORB glasses and their implications for mantle melting. Geochimica et Cosmochimica Acta 69, 711–725.
Bina, C.R., Helffrich, G., 1994. Phase transition Clapeyron slopes and transition zone seismic discontinuity topography. Journal of Geophysical Research 99, 15853–15860.
Blatter, D.L., Carmichael, I.S.E., 2001. Hydrous phase equilibria of a Mexican high-silica andesite; a candidate for a mantle origin? Geochimica et Cosmochimica Acta 65, 4043–4065.
Bock, G., 1991. Long-period S to P converted waves and the onset of partial melting beneath Oahu, Hawaii. Geophysical Research Letters 18, 869–872.
Bonatti, E., 1990. Not so hot "hot spots" in the oceanic mantle. Science 250, 107–111.
Bowen, N.L., Anderson, O., 1914. The binary system MgO–SiO2. American Journal of Science 37, 487–500.
Brandon, A.D., Norman, M.D., Walker, R.J., Morgan, J.W., 1999. ^{186}Os–^{187}Os systematics of Hawaiian picrites. Earth and Planetary Science Letters 174, 25–42.
Cammarano, F., Goes, S., Vacher, P., Giardini, D., 2003. Inferring upper mantle temperatures from seismic velocities. Physics of the Earth and Planetary Interiors 138, 197–222.
Cawthorn, R.G., 1975. Degrees of melting in mantle diapers and the origin of ultrabasic liquids. Earth and Planetary Science Letters 27, 113–120.
Christiansen, R.L., Foulger, G.R., Evans, J.R., 2002. Upper-mantle origin of the Yellowstone hotspot. Geological Society of America Bulletin 114, 1245–1256.
Clague, D.A., Weber, W.S., Dixon, J.E., 1991. Picritic glasses from Hawaii. Nature 353, 553–556.
Da Silva, C.R.S., Wentzcovitch, R.M., Patel, A., Price, G.D., Karato, S.I., 2000. The composition and geotherm of the lower mantle: constraints from the elasticity of silicate perovskite. Physics of the Earth and Planetary Interiors 118, 103–109.
Dalton, J.A., Presnall, D.C., 1998a. The continuum of primary carbonatitic–kimberlitic melt compositions in equilibrium with lherzolite: data from the system $CaO–MgO–Al_2O_3–SiO_2–CO_2$ at 6 GPa. Journal of Petrology 39, 1953–1964.
Dalton, J.A., Presnall, D.C., 1998b. Carbonatitic melts along the solidus of model lherzolite in the system $CaO–MgO–Al_2O_3–SiO_2–CO_2$ from 3 to 7 GPa. Contributions to Mineralogy and Petrology 131, 123–135.
Davies, G.F., 1999. Dynamic Earth: Plates, Plumes and Mantle Convection. Cambridge University Press. 458 pp.
Dixon, J.E., Leist, L., Langmuir, C., Schilling, J.-G., 2002. Recycled dehydrated lithosphere observed in plume-influenced mid-ocean-ridge basalt. Nature 420, 385–389.
Doglioni, C., Green, D.H., Mongelli, F., 2005. On the shallow origin of hotspots and the westward drift of the lithosphere. In: Foulger, G.R., Natland, J.H., Presnall, D.C., Anderson, D.L. (Eds.), Plates, Plumes and Paradigms. Geological Society of America Special Paper, vol. 388, pp. 735–750.
Draper, D.S., Johnston, A.D., 1992. Anhydrous PT phase relations of an Aleutian high-MgO basalt; an investigation of the role of olivine-liquid reaction in the generation of arc high-alumina basalts. Contributions to Mineralogy and Petrology 112, 501–519.
Dunn, T., Sen, C., 1994. Mineral/matrix partition coefficient for orthopyroxene, plagioclase, and olivine in basaltic to andesitic systems: a combined analytical and experimental study. Geochimica et Cosmochimica Acta 58, 717–733.
Eissen, J.P., 1982, Petrologie comparee de basalts de differents segments de zones d'accreion oceanique e taux d'accretion varies (Mer Rouge, Atlantique, Pacifique), These, U. Strausberg.
Elthon, D., Scarfe, C.M., 1984. High-pressure phase equilibria of a high-magnesia basalt and the genesis of primary oceanic basalts. American Mineralogist 69, 1–15.
Esperança, S., Holloway, J.R., 1987. On the origin of some mica-lamprophyres; experimental evidence from a mafic minette. Contributions to Mineralogy and Petrology 95, 207–216.
Falloon, T.J., Green, D.H., 1987. Anhydrous partial melting of MORB pyrolite and other peridotite compositions at 10 kbar; implications for the origin of primitive MORB glasses. Mineralogy and Petrology 37, 181–219.
Falloon, T.J., Green, D.H., Hatton, C.J., Harris, K.L., 1988. Anhydrous partial melting of a fertile and depleted peridotite from 2 to 30 Kb and application to basalt petrogenesis. Journal of Petrology 29, 1257–1282.
Falloon, T.J., Green, D.H., O-Neill, H.-St., Hibberson, W.O., 1997. Experimental tests of low degree peridotite partial melt compositions;

implications for the nature of anhydrous near-solidus peridotite melts at 1 GPa. Earth and Planetary Science Letters 152, 149–162.

Falloon, T.J., Danyushevsky, L.V., Green, D.H., 2001. Peridotite melting at 1 GPa; reversal experiments on partial melt compositions produced by peridotite-basalt sandwich experiments. Journal of Petrology 42, 2363–2390.

Feigenson, M.D., Bolge, L.L., Carr, M.J., Herzberg, C.T., 2003. REE inverse modeling of HSDP2 basalts: evidence for multiple sources in the Hawaiian plume. Geochemistry, Geophysics, Geosystems 4 (2), 8706. doi:10.1029/2001GC000271.

Ford, C.E., Russell, D.G., Craven, J.A., Fisk, M.R., 1983. Olivine-liquid equilibria: temperature, pressure and composition dependence of the crystal/liquid cation partition coefficients for Mg, Fe^{2+}, Ca and Mn. Journal of Petrology 24, 256–265.

Foulger, G.R., Natland, J.H., 2003. Is "hotspot" volcanism a consequence of plate tectonics? Science 300, 921–922.

Foulger, G.R., Pritchard, M.J., Julian, B.R., Evans, J.R., Allen, R.M., Nolet, G., Morgan, W.J., Bergsson, B.H., Erlendsson, P., Jakobsdottir, S., Ragnarsson, S., Stefansson, R., Vogfjord, K., 2000. The seismic anomaly beneath Iceland extends does to the mantle transition zone and no deeper. Geophysical Journal International 142, F1–F5.

Foulger, G.R., Natland, J.H., Anderson, D.L., 2005. Genesis of the Iceland melt anomaly by plate tectonic processes. In: Foulger, G.R., Natland, J.H., Presnall, D.C., Anderson, D.L. (Eds.), Plates, Plumes and Paradigms. Geological Society of America Special Paper, vol. 388, pp. 595–626.

Fram, M.S., Lesher, C.E., 1997. Generation and polybaric differentiation of east Greenland early Tertiary flood basalts. Journal of Petrology 38, 231–275.

Fram, M.S., Longhi, J., 1992. Phase equilibria of dikes associated with Proterozoic anorthosite complexes. American Mineralogist 77, 605–616.

Frost, D.J., 2003. The structure and sharpness of $(Mg,Fe)_2SiO_4$ phase transformations in the transition zone. Earth and Planetary Science Letters 216, 313–328.

Gaetani, G.A., Grove, T.L., 1998. The influence of melting of mantle peridotite. Contributions to Mineralogy and Petrology 131, 323–346.

Garcia, M.O., 2002. Submarine picritic basalt from Ko'olau volcano, Hawai'i: implications for parental magma composition and mantle source. In: Takahashi, E., Lipman, P.W., Garcia, M.O., Naka, J., Aramaki, S. (Eds.), Hawaiian Volcanoes: Deep Underwater Perspectives. Geophysical Monograph, vol. 128. AGU, Washington DC, pp. 391–402.

Garcia, M.O., Hulsebosch, T.P., Rhodes, J.M., 1995. Olivine-rich submarine basalts from the southwest rift zone of Mauna Loa volcano: implications for magmatic processes and geochemical evolution. In: Rhodes, J.M., Lockwood, J.P. (Eds.), Mauna Loa Revealed. Geophysical Monograph, vol. 92. AGU, Washington DC, pp. 219–240.

Gee, L.L., Sack, R.O., 1988. Experimental petrology of melilite nephelinites. Journal of Petrology 29, 1233–1255.

Ghiorso, M.S., Carmichael, I.S.E., Rivers, M.L., Sack, R.O., 1983. The Gibbs free energy of natural silicate liquids; an expanded regular solution approximation for the calculation of magmatic intensive variables. Contributions to Mineralogy and Petrology 84, 107–145.

Green, D.H., Falloon, T.J., 2005. Primary magmas at mid-ocean ridges, "hot spots" and other intraplate settings; constraints on mantle potential temperature. In: Foulger, G.R., Natland, J.H., Presnall, D.C., Anderson, D.L. (Eds.), Plates, Plumes and Paradigms. Geological Society of America Special Paper, vol. 388, pp. 217–248.

Green, D.H., Ringwood, A.E., 1967. The genesis of basaltic magmas. Contributions to Mineralogy and Petrology 15, 103–190.

Green, D.H., Falloon, T.J., Eggins, S.M., Yaxley, G.M., 2001. Primary magmas and mantle temperatures. European Journal of Mineralogy 13, 437–451.

Grove, T.L., Juster, T.C., 1989. Experimental investigations of low-Ca pyroxene stability and olivine-pyroxene-liquid equilibria at 1-atm in natural basaltic and andesitic liquids. Contributions to Mineralogy and Petrology 103, 287–305.

Grove, T.L., Kinzler, R.J., Bryan, W.B., 1990. Natural and experimental phase relations of lavas from Serocki Volcano. Proceedings of the Ocean Drilling Program. Scientific Results 106/109, 9–17.

Grove, T.L., Kinzler, R.J., Bryan, W.B., 1992, Fractionation of mid-ocean ridge basalt (MORB). In: Phipps Morgan, J., Blackman, D.K. Sinton, J.M. (Eds.), Mantle flow and melt generation at mid ocean ridges. Geophys. Monogr. Ser., 7, Am. Geophys. Union., pp. 281–310.

Grove, T.L., Donnelly-Nolan, J.M., Housh, T., 1997. Magmatic processes that generated the rhyolite of Glass Mountain, Medicine lake volcano. N. California. Contributions to Mineralogy and Petrology 127, 205–223.

Grove, T.L., Elkins-Tanton, L.T., Parman, S.W., Chatterjee, N., Muntener, O., Gaetani, G.A., 2003. Fractional crystallization and mantle-melting controls on calk–alkaline differentiation trends. Contributions to Mineralogy and Petrology 145, 515–533.

Gudfinnsson, G.H., Presnall, D.C., 2000. Melting behavior of model lherzolite in the system $CaO–MgO–Al_2O_3–SiO_2–FeO$ at 0.7–2.8 GPa. Journal of Petrology 41, 1241–1269.

Gudfinnsson, G.H., Presnall, D.C., 2001. A pressure-independent geothermometer for primitive mantle melts. Journal of Geophysical Research 106, 16205–16211.

Hays, M.R., Perfit, M.R., Fornari, D.J., Ridley, W., 2004. Magmatism in the Siqueiros transform: major and trace element evidence for mixing and multiple sources. Trans. Am. Geophys. Union, T41A-1165.

Herzberg, C., 1995. Generation of plume magmas through time: an experimental perspective. Chemical Geology 126, 1–16.

Herzberg, C., 2004. Geodynamic information in peridotite petrology. Journal of Petrology 45, 2507–2530.

Herzberg, C., O'Hara, M.J., 1998. Phase equilibrium constraints on the origin of basalts, picrites and komatiites. Earth-Science Reviews 44, 39–79.

Herzberg, C., O'Hara, M.J., 2002. Plume-associated ultramafic magmas of Phanerozoic age. Journal of Petrology 43, 1857–1883.

Herzberg, C., Zhang, J., 1996. Melting experiments on anhydrous peridotite KLB-1; composition of magmas in the upper mantle and transition zone. Journal of Geophysical Research 101, 8271–8295.

Hess, H.H., 1962. History of the ocean basins. In: Engel, A.E., James, H.L., Leonard, B.F. (Eds.), Petrologic studies: A volume in honor of A.F. Buddington. Geological Society of America, pp. 599–620.

Hirose, K., 2002. Phase transitions in pyrolitic mantle around 670-km depth: implications for upwelling of plumes from the lower mantle. Journal of Geophysical Research 107, 2078. doi:10.1029/2001JB000597.

Hirschmann, M.M., 2000. Mantle solidus: experimental constraints and the effects of peridotite composition. Geochemistry, Geophysics, Geosystems 1 (2000GC000070).

Hofmeister, A.M., 1999. Mantle values of thermal conductivity and the geotherm from phonon lifetimes. Science 283, 1699–1706.

Humphreys, E.D., Dueker, K.G., Schutt, D.L., Smith, R.B., 2000. Beneath Yellowstone: evaluating plume and nonplume models using teleseismic images of the upper mantle. GSA Today 10, 1–7.

Humayun, M., Qin, L., Norman, M.D., 2004. Geochemical evidence for excess Iron in the mantle beneath Hawaii. Science 306, 91–94.

Ito, E., Katsura, T., 1989. A temperature profile of the mantle transition zone. Geophysical Research Letters 16, 425–428.

Ito, G., Shen, Y., Hirth, G., Wolfe, C.J., 1999. Mantle flow, melting, and dehydration of the Iceland mantle plume. Earth and Planetary Science Letters 165, 81–96.

Jackson, E.D., Shaw, H.R., Bargar, K.E., 1975. Calculated geochronology and stress field orientation along the Hawaiian chain. Earth and Planetary Science Letters 26, 145–155.

Jacques, A.L., Green, D.H., 1980. Anhydrous melting of peridotite at 0–15 kb pressure and the genesis of tholeiitic basalts. Contributions to Mineralogy and Petrology 73, 210–287.

Jeanloz, R., Morris, S., 1986. Temperature distribution in the crust and mantle. Annual Review of Earth and Planetary Sciences 14, 377–415.

Jeanloz, R., Thompson, A.B., 1983. Phase transitions and mantle discontinuities. Reviews of Geophysics and Space Physics 21, 51–74.

Juster, T.C., Grove, T.L., Perfit, M.R., 1989. Experimental constraints on the generation of FeTi basalts, andesites and rhyodacites at the Galapagos Spreading center, 85°W and 95°W. Journal of Geophysical Research 94, 9251–9274.

Kelemen, P.B., Koga, K., Shimuzu, N., 1997. Geochemistry of gabbro sills in the crust–mantle transition zone of the Oman ophiolite: implications for the origin of the oceanic lower crust. Earth and Planetary Science Letters 146, 475–488.

King, S.D., 1995. Models of mantle viscosity, A Handbook of Physical Constants. American Geophysical Union Ref. Shelf 2, 227–236.

Kinzler, R.J., Grove, T.L., 1985. Crystallization and differentiation of Archean komatiite lavas from Northeast Ontario; phase equilibrium and kinetic studies. American Mineralogist 70, 40–51.

Kinzler, R.J., Grove, T.L., 1992a. Primary magmas of mid-ocean ridge basalts 1. Experiments and methods. Journal of Geophysical Research 97, 6885–6906.

Kinzler, R.J., Grove, T.L., 1992b. Primary magmas of mid-ocean ridge basalts 2. Applications. Journal of Geophysical Research 97, 6907–6926.

Klein, E.M., Langmuir, C.H., 1987. Global correlations of ocean ridge basalt chemistry with axial depth and crustal thickness. Journal of Geophysical Research 92, 8089–8115.

Klügel, A., Klein, F., 2006. Complex magma storage and ascent at embryonic submarine volcanoes from Madeira Archipelago. Geology 34, 337–340.

Kogiso, T., Hirose, K., Takahashi, E., 1998. Melting experiments on homogeneous mixtures of peridotite and basalt; application to the genesis of ocean island basalts. Earth and Planetary Science Letters 162, 45–61.

Kogiso, T., Hirschmann, M.M., 2001. Experimental study of clinopyroxenite partial melting and the origin of ultra-calcic melt inclusions. Contributions to Mineralogy and Petrology 142 (3), 347–360.

Kress, V.C., Carmichael, I.S.E., 1988. Stoichiometry of the iron oxidation reaction in silicate melts. American Mineralogist 73, 1267–1274.

Langmuir, C.H., Hanson, G.N., 1980. An evaluation of major element heterogeneity in the mantle sources of basalts. Philosophical Transactions of the Royal Society of London. A 297, 383–407.

Langmuir, C.H., Hanson, G.N., 1981. Calculating mineral-melt equilibria with stoichiometry, mass balance, and single component distribution coefficients, in Thermodynamics of Minerals and Melts. In: Newton, R.C., Navrotsky, A., Wood, B.J. (Eds.), Springer-Verlag, pp. 247–271.

Langmuir, C.H., Klein, E.M., Plank, T., 1992. Petrological systematics of mid-ocean ridge basalts: constraints on melt generation beneath ocean ridges. In: Morgan, J.P., Blackman, D.K., Sinton, J.M. (Eds.), Mantle Flow and Melt Generation at Mid-Ocean Ridges. Geophysical Monograph, vol. 71. AGU, Washington DC, pp. 183–280.

Laske, G., Morgan, J.P., Orcutt, J.A., 1999. First results from the Hawaiian SWELL Plot Experiment. Geophysical Research Letters 26, 3397–3400.

Leitch, A.M., Steinbach, V., Yuen, D.A., 1996. Centerline temperature of mantle plumes in various geometries: incompressible flow. Journal of Geophysical Research 101, 21829–21846.

Leeman, W.P., Lewis, J.F., Evarts, R.C., Conrey, R.M., Streck, M.J., 2005. Petrologic constraints on the thermal structure of the Cascades arc. Journal of Volcanology and Geothermal Research 140, 67–105.

Li, X., Kind, R., Yuan, X., Wölbern, I., Hanka, W., 2004. Rejuvenation of the lithosphere by the Hawaiian plume. Nature 427, 827–829.

Longhi, J., 2002. Some phase equilibrium systematics of lherzolite melting: I. Geochemistry, Geophysics, Geosystems 3. doi:10.1029/2001GC000204.

Longhi, J., 2005. Temporal stability an pressure calibration of barium carbonate and talc/pyrex pressure media in a piston-cylinder apparatus. American Mineralogist 90, 206–218.

Longhi, J., Pan, V., 1988. A reconnaissance study of phase boundaries in low-alkali basaltic liquids. Journal of Petrology 29, 115–147.

Longhi, J., Walker, D., Hays, J.F., 1978. The distribution of Fe and Mg between olivine and lunar basaltic liquids. Geochimica et Cosmochimica Acta 42, 1545–1558.

Longhi, J., Vander Auwera, J., Fram, M.S., Duchesne, J.-C., 1999. Some phase equilibrium constraints on the origin of Proterozoic (massif) anorthosites and related rocks. Journal of Petrology 40, 339–362.

MacLennan, J., McKenzie, D., Gronvold, K., 2001a. Plume-driven upwelling under central Iceland. Earth and Planetary Science Letters 194, 67–82.

MacLennan, J., McKenzie, D.M., Gronvöld, K., Slater, L., 2001b. Crustal accretion under northern Iceland. Earth and Planetary Science Letters 191, 295–310.

McKenzie, D., 1967. Some remarks on heat flow and gravity anomalies. Journal of Geophysical Research 72, 6261–6273.

McKenzie, D., 1984. The generation and compaction of partially molten rock. Journal of Petrology 25, 713–765.

McKenzie, D., Bickle, M.J., 1988. The volume and composition of melt generated by extension of the lithosphere. Journal of Petrology 29, 625–679.

MELT Seismic Team, 1998. Imaging the deep seismic structure beneath a mid-ocean ridge: the MELT experiment. Science 280, 1215–1218.

Montelli, R., Nolet, G., Dahlen, F.A., Masters, G., Engdahl, E.R., Hung, S.-H., 2004. Finite-frequency tomography reveals a variety of plumes in the mantle. Science 303, 338–343.

Montierth, C., Johnston, A.D., Cashman, K.V., 2000. An empirical glass-composition-based geothermometer for Mauna Loa lavas. In: Rhodes, J.M., Lockwood, J.P. (Eds.), Mauna Loa Revealed. Geophysical Monograph, vol. 92. AGU, Washington DC, pp. 207–218.

Moore, G., Carmichael, I.S.E., 1998. The hydrous phase equilibria (to 3 kbar) of an andesite and basaltic andesite from western Mexico; constraints on water content and conditions of phenocryst growth. Contributions to Mineralogy and Petrology 130, 304–319.

Morgan, W.J., 1971. Convection plumes in the lower mantle. Nature 230, 42–43.

Müntener, O., Kelemen, P.B., Grove, T.L., 2001. The role of H_2O during crystallization of primitive arc magmas under uppermost mantle conditions and genesis of igneous pyroxenites: and

experimental study. Contributions to Mineralogy and Petrology 141, 643–658.
Murck, B.W., Campbell, I.H., 1986. The effects of temperature, oxygen fugacity and melt composition on the behavior of chromium in basic and ultrabasic melts. Geochimica et Cosmochimica Acta 50, 1871–1887.
Nataf, H.-C., VanDecar, J., 1993. Seismological detection of a mantle plume? Nature 364, 115–120.
Norman, M.D., Garcia, M.O., 1999. Primitive magmas and source characteristics of the Hawaiian plume: petrology and geochemistry of shield picrites. Earth and Planetary Science Letters 168, 27–44.
Norman, M.D., Garcia, M.O., Kamenetsky, V.S., Nielsen, R.L., 2002. Olivine-hosted melt inclusions in Hawaiian picrites: equilibration, melting and plume source characteristics. Chemical Geology 183, 143–168.
O'Hara, M.J., 1968. Are ocean floor basalts primary magma? Nature 220, 683–686.
O'Hara, M.J., 1970. Upper mantle composition inferred from laboratory experiments and observation of volcanic products. Physics of Earth and Planetary Interiors 3, 236–245.
O'Hara, M.J., 1978. Thermal history of magmas; the low pressure reference point. Philosophical transactions of the Royal Society of London 288A, 627–629.
Parman, S.W., Dann, J.C., Grove, T.L., de-Wit, M.J., 1997. Emplacement conditions of komatiite magmas from the 3.49 Ga Komati Formation, Barberton greenstone belt, South Africa. Earth and Planetary Science Letters 150, 303–323.
Perfit, M.R., Fornari, D.J., Ridley, W.I., Kirk, P.D., Casey, J., Kastens, K.A., Reynolds, J.R., Edwards, M., Desonie, D., Shuster, R., Paradis, S., 1996. Recent volcanism in the Siqueiros transform fault: picritic basalts and implications for MORB magma genesis. Earth and Planetary Science Letters 141, 91–108.
Pichavant, M., Mysen, B.O., Macdonald, R., 2002. Source and H_2O content of high-MgO magmas in island arc settings: an experimental study of primitive calc–alkaline basalt from St. Vincent, Lesser Antilles arc. Geochimica et Cosmochimica Acta 66, 2193–2209.
Pickering-Witter, J., Johnston, A.D., 2000. The effects of variable bulk composition on the melting systematics of fertile peridotitic assemblages. Contributions to Mineralogy and Petrology 140, 190–211.
Powers, H.A., 1955. Composition and origin of basaltic magma of the Hawaiian Islands. Geochimica et Cosmochimica Acta 7, 77–107.
Presnall, D.C., Gudfinnsson, G.H., 2005. Carbonate-rich melts in the oceanic low-velocity zone and deep mantle. In: Foulger, G.R., Natland, J.H., Presnall, D.C., Anderson, D.L. (Eds.), Plates, Plumes and Paradigms. Geological Society of America Special Paper, vol. 388, pp. 207–216.
Presnall, D.C., Walter, M.J., 1993. Melting of forsterite, Mg_2SiO_4, from 9.7 to 16.5 GPa. Journal of Geophysical Research 98, 19777–19783.
Presnall, D.C., Gudfinnsson, G.H., Walter, M.J., 2002. Generation of mid-ocean ridge basalts at pressures from 1 to 7 GPa. Geochmicia et Cosmochimica Acta 66, 2073–2090.
Priestley, K., Tilmann, F., 1999. Shear-wave structure of the lithosphere above the Hawaiian hot spot from two-station Rayleigh wave phase velocity measurements. Geophysical Research Letters 26, 1493–1496.
Putirka, K., 1997. Magma transport at Hawaii: inferences based on igneous thermobarometry. Geology 25, 69–72.
Putirka, K., 1998. Garnet+liquid equilibrium. Contributions to Mineralogy and Petrology 131, 273–288.
Putirka, K., 1999. Melting depths and mantle heterogeneity beneath Hawaii and the East Pacific Rise: constraints from Na/Ti and rare earth element ratios. Journal of Geophysical Research 104, 2817–2829.
Putirka, K., 2005. Mantle potential temperatures at Hawaii, Iceland, and the mid-ocean ridge system, as inferred from olivine phenocrysts: evidence for thermally-driven mantle plumes. Geochemistry, Geophysics, Geosystems. doi:10.1029/2005GCGC000915.
Rhodes, J.M., Vollinger, M.J., 2004. Composition of basaltic lavas sampled by phase-2 of the Hawaii Scientific Drilling Project: geochemical stratigraphy and magma series types. Geochemistry, Geophysics, Geosystems 5 (3). doi:10.1029/2002GC00434.
Rhodes, J.M., Vollinger, M.J., 2005. Ferrous/ferric ratios in 1984 Mauna Loa lavas: a contribution to understanding the oxidation state of Hawaiian magmas. Contributions to Mineralogy and Petrology 149, 666–674.
Ribe, N.M., Christensen, U.R., 1999. The dynamical origin of Hawaiian volcanism. Earth and Planetary Science Letters 171, 517–531.
Righter, K., Carmichael, I.S.E., 1996. Phase equilibria of phlogopite lamprophyres from western Mexico; biotite-liquid equilibria and *P–T* estimates for biotite-bearing igneous rocks. Contributions to Mineralogy and Petrology 123 (1), 1–21.
Ritsema, J., Allen, R.M., 2003. The elusive mantle plume. Earth and Planetary Science Letters 207, 1–12.
Robinson, J.A.C., Wood, B.J., Blundy, J.D., 1998. The beginning of melting of fertile and depleted peridotite at 1.5 GPa. Earth and Planetary Science Letters 155, 97–111.
Roeder, P.L., Emslie, R.F., 1970. Olivine-liquid equilibrium. Contributions to Mineralogy and Petrology 29, 275–289.
Sack, R.O., Walker, D., Carmichael, I.S.E., 1987. Experimental petrology of alkalic lavas: constraints on cotectics of multiple saturation in natural basic liquids. Contributions to Mineralogy and Petrology 96, 1–23.
Salters, V.J.M., Hart, S.R., 1989. The Hf paradox and the role of garnet in the source of mid-ocean ridge basalts. Nature 342, 420–422.
Schilling, J.G., 1991. Fluxes and excess temperatures of mantle plumes inferred from their interaction with migrating mid-ocean ridges. Nature 352, 397–403.
Schwab, B.E., Johnston, A.D., 2001. Melting systematics of modally variable, compositionally intermediate peridotites and the effects of mineral fertility. Journal of Petrology 42, 1789–1811.
Shaw, H.R., Jackson, E.D., 1973. Linear island chains in the Pacific: results o thermal plumes or gravitational anchors? Journal of Geophysical Research 78, 8634–8652.
Shen, Y., Forsyth, D.W., 1995. Geochemical constraints on initial and final depths of melting beneath mid-ocean ridges. Journal of Geophysical Research 100, 2211–2237.
Sisson, T.W., Grove, T.L., 1993a. Experimental investigations of the role of H_2O in calc–alkaline differentiation and subduction zone magmatism. Contributions to Mineralogy and Petrology 113, 143–166.
Sisson, T.W., Grove, T.L., 1993b. Temperatures and H_2O contents of low-MgO high-alumina basalts. Contributions to Mineralogy and Petrology 113, 167–184.
Sleep, N.H., 1990. Hotspots and mantle plumes: some phenomenology. Journal of Geophysical Research 95, 6715–6736.
Smyth, J.R., Frost, D., 2002. The effect of water on the 410-km discontinuity; an experimental study. Geophysical Research Letters 29, 10–13.
Sobolev, A.V., Danyushevsky, L.V., 1994. Petrology and geochemistry of boninites from the north termination of the Tonga Trench: constraints on the generation conditions of primary high-Ca boninite magmas. Journal of Petrology 35, 1183–1211.

Sobolev, A.V., Hofmann, A.W., Sobolev, S.V., Nikogosian, I.K., 2005. An olivine-free mantle source of Hawaiian shield basalts. Nature 434, 590–597.

Stein, C.A., Stein, S., 1992. A model for the global variation in oceanic depth and heat flow with lithospheric age. Nature 359, 123–129.

Stolper, E., 1980. A phase diagram for mid-ocean ridge basalts: preliminary results and implications for petrogenesis. Contributions to Mineralogy and Petrology 74, 13–27.

Stracke, A., Salters, V.J.M., Sims, K.W., 2003. Assessing the presence of garnet–pyroxenite in the mantle sources of basalts through combined hafnium–neodymium–thorium isotope systematics. Geochemistry, Geophysics, Geosystems 1 (1999GC000013).

Sugawara, T., 2000. Empirical relationships between temperature, pressure, and MgO content in olivine and pyroxene saturated liquid. Journal of Geophysical Research 105, 8457–8472.

Sugawara, T., 2001. Ferric iron partitioning between plagioclase and silicate liquid; thermodynamics and petrological applications. Contributions to Mineralogy and Petrology 141, 659–686.

Tackley, P.J., 2000. Mantle convection and plate tectonics: toward an integrated physical and chemical model. Science 288, 2002–2007.

Takagi, D., Sato, H., Nakagawa, 2005. Experimental study of a low-alkali tholeiite at 1–5 kbar: optimal condition for the crystallization of high-An plagioclase in hydrous arc tholeiite. Contributions to Mineralogy and Petrology 149, 527–540.

Takahashi, E., Shimazaki, T., Tsuzaki, Y., Yoshida, H., 1993. Melting study of a peridotite KLB-1 to 6.5 GPa, and the origin of basaltic magmas. Philosophical Transactions of the Royal Society of London 342, 105–120.

Thompson, R.N., Discussion, Bottinga, Y., Allegre, C.J. 1978. Partial melting under spreading ridges, Philosophical Transactions of the Royal Society of London, 288A, 524–525.

Thy, P., 1991. High and low pressure phase equilibria of a mildly alkalic lava from the 1965 Surtsey eruption: experimental results. Lithos 26, 223–243.

Thybo, H., Nielsen, L., Perchuc, E., 2003. Seismic scattering at the top of the mantle transition zone. Earth and Planetary Science Letters 216, 259–269.

Toplis, M.J., 2005. The thermodynamics of iron and magnesium partitioning between olivine and liquid: criteria for assessing and predicting equilibrium in natural and experimental systems. Contributions to Mineralogy and Petrology 149, 22–39.

Tormey, D.R., Grove, T.L., Bryan, W.B., 1987. Experimental petrology of normal MORB near the Kane Fracture Zone: 22°–25° N, mid-Atlantic Ridge. Contributions to Mineralogy and Petrology 96, 121–139.

Trönnes, R.G., Canil, D., Wei, K., 1992. Element partitioning between silicate minerals and coexisting melts at pressure of 1–27 GPa, and implications for mantle evolution. Earth and Planetary Science Letters 111, 241–255.

Vander Auwera, J., Longhi, J., 1994. Experimental study of jotunite (hypersthene monzodiorite): constraints on the parent magma composition and crystallization conditions (P, T, fO2) of the Bjerkreim–Sokndal layered intrusion (Norway). Contributions to Mineralogy and Petrology 118, 60–78.

Vander Auwera, J., Longhi, J., Duchesne, J.-C., 1998. A liquid line of descent of the jotunite (hypersthene monzodiorite) suite. Journal of Petrology 39, 439–468.

Verhoogen, J., 1954. Petrological evidence on temperature distribution in the mantle of the earth. Transaction of the American Geophysical Union 35, 85–92.

Verhoogen, J., 1965. Phase changes and convection in the Earth's mantle. Philosophical Transactions of the Royal Society of London 258A, 276–283.

Verhoogen, J., 1973. Possible temperatures in the oceanic upper mantle and the formation of magma. Geological Society of America Bulletin 84, 515–522.

Wagner, T.P., Grove, T.L., 1997. Experimental constraints on the origin of lunar high-Ti ultramafic glasses. Geochimica et Cosmochimica Acta 61, 1315–1327.

Walker, D., 2000. Core participation in mantle geochemistry: geochemical Society Ingerson Lecture, GSA, Denver, October 1999. Geochimica et Cosmochimica Acta 64, 2897–2911.

Walker, D., Shibata, T., DeLong, St.E., 1979. Abyssal tholeiites from the Oceanographer fracture zone; II, Phase equilibria and mixing. Contributions to Mineralogy and Petrology 70, 111–125.

Walker, D., Clark, S.M., Cranswick, L.M.D., Johnson, M.C., Jones, R.L., 2002. O_2 volumes at high pressure from $KClO_4$ decomposition: D'' as a siderophile element pump instead of a lid on the core. Geochemistry, Geophysics, Geosystems 3. doi:10.1029/2001GC000225.

Walter, M.J., 1998. Melting of garnet peridotite and the origin of komatiite and depleted lithosphere. Journal of Petrology 39, 29–60.

Wang, K., Plank, T., Walker, J.D., Smith, E.I., 2002. A mantle melting profile across the Basin and Range, SW USA. Journal of Geophysical Research 107. doi:10.1029/2001JB000209.

Wasylenki, L.E., Baker-, M.B., Kent, A.J.R., Stolper, E.M., 2003. Near-solidus melting of the shallow upper mantle; partial melting experiments on depleted peridotite. Journal of Petrology 44, 1163–1191.

Watson, S., McKenzie, D., 1991. Melt generation by plumes; a study of Hawaiian volcanism. Journal of Petrology 32, 501–537.

Wolfe, C.J., Bjarnason, I.Th., VanDecar, J.C., Solomon, S.C., 1997. Seismic structure of the Iceland mantle plume. Nature 385, 245–247.

Wright, T.L., 1973. Magma mixing as illustrated by the 1959 eruption, Kilauea volcano, Hawaii. Geological Society of America Bulletin 84, 849–858.

Wyllie, P.J., 1988, Solidus Curves, mantle plumes, and magma generation beneath Hawaii, 93, 4171–4181.

Xirouchakis, D., Hirschmann, M.M., Simpson, J.A., 2001. The effect of titanium on the silica content and on mineral-liquid partitioning of mantle-equilibrated melts. Geochimica et Cosmochimica Acta 65, 2201–2217.

Yang, H.-J., Kinzler, R.J., Grove, T.L., 1996. Experiments and models of anhydrous, basaltic olivine–plagioclase–augite saturated melts from 0.001 to 10 kbar. Contributions to Mineralogy and Petrology 124, 1–18.